Cell Biology

Septins function in exocytosis via physical interactions with the exocyst complex in fission yeast cytokinesis

Reviewed Preprint
v1 • September 4, 2024
Not revised

Davinder Singh, Yajun Liu, Yi-Hua Zhu, Sha Zhang, Shelby Naegele, Jian-Qiu Wu

Department of Molecular Genetics, The Ohio State University, Columbus, United States • Department of Biological Chemistry and Pharmacology, The Ohio State University, Columbus, United States

Abstract

Septins can function as scaffolds for protein recruitment, membrane-bound diffusion barriers, or membrane curvature sensors. Septins are important for cytokinesis, but their exact roles are still obscure. In fission yeast, four septins (Spn1 to Spn4) accumulate at the rim of the division plane as rings. The octameric exocyst complex, which tethers exocytic vesicles to the plasma membrane, exhibits a similar localization and is essential for plasma membrane deposition during cytokinesis. Without septins, the exocyst spreads across the division plane but absent from the rim during septum formation. These results suggest that septins and the exocyst physically interact for proper localization. Indeed, we predicted six pairs of direct interactions between septin and exocyst subunits by AlphaFold2 ColabFold, most of them are confirmed by co-immunoprecipitation and yeast two-hybrid assays. Exocyst mislocalization results in mistargeting of secretory vesicles and their cargos, which leads to cell-separation delay in septin mutants. Our results indicate that septins guide the targeting of exocyst complex on the plasma membrane for vesicle tethering during cytokinesis through direct physical interactions.

eLife assessment

How secretion is regulated during cell division and how membrane trafficking factors cooperate with the cytoskeleton during cell division remain poorly understood. In this work the authors find potential direct interactions between the polymeric septin cytoskeleton and the exocyst complex, using fission yeast as a model organism. The work provides a **valuable** body of new information that will be of great interest to the cell biology community. The evidence is strong and rigorous in many places but is **incomplete** in other respects.

https://doi.org/10.7554/eLife.101113.1.sa3

Introduction

Septins are a family of GTP-binding proteins that are highly conserved from yeast to mammalian cells, but absent in land plants (Longtine et al., 1996; Gladfelter et al., 2001; Cao et al., 2007; Nishihama et al., 2011; Onishi and Pringle, 2016; Marquardt et al., 2019; Woods and Gladfelter, 2021). They form hetero-oligomeric complexes that can assemble into different higher-order structures such as rings, gauzes, hourglasses, and carry out various functions (Frazier et al., 1998; Hsu et al., 1998; Kinoshita, 2003; Sheffield et al., 2003; Bertin et al., 2008; Garcia et al., 2011; Bridges et al., 2014). Septins can serve as scaffolds for protein recruitment at discrete cellular locations (Gladfelter et al., 2001; Versele and Thorner, 2005; Mostowy and Cossart, 2012; Finnigan et al., 2015; Meitinger and Palani, 2016; Perez et al., 2016; Marquardt et al., 2019). Septins are proposed to act as a diffusion barrier to ensure that cellular components are spatially segregated or compartmentalized (Dobbelaere and Barral, 2004; Caudron and Barral, 2009; Hu and Nelson, 2011; McMurray et al., 2011). They can also sense the membrane curvatures and/or deform the plasma membrane due to their lipid-binding properties (Bridges and Gladfelter, 2016; Cannon et al., 2017; Cannon et al., 2019; McMurray, 2019; Shi et al., 2023). The diverse roles of septins lead to their involvement in multiple processes including cytokinesis, mitosis, exocytosis, apoptosis, fungal or viral infections, neuronal spine morphogenesis, ciliogenesis, and spermiogenesis (Longtine et al., 1996; Kartmann and Roth, 2001; Mostowy and Cossart, 2012; Dolat et al., 2014; Momany and Talbot, 2017; Ageta-Ishihara and Kinoshita, 2021; Neubauer and Zieger, 2021; Woods and Gladfelter, 2021; Safavian et al., 2023).

One of the best-studied septin functions is their roles in cytokinesis in the budding yeast *Saccharomyces cerevisiae* (Hartwell, 1971; Haarer and Pringle, 1987; Ford and Pringle, 1991; Kim et al., 1991; DeMarini et al., 1997; Bi et al., 1998; Lippincott and Li, 1998; Longtine et al., 1998). The septin ring or hourglass structures at the presumptive bud site and bud neck are required for the recruitment and maintenance of various cytokinesis proteins (Bi et al., 1998; Lippincott and Li, 1998; Gladfelter et al., 2001; Longtine and Bi, 2003; Marquardt et al., 2019).

These roles occur through either direct interactions with proteins such as the F-BAR protein Hof1 (Vallen et al., 2000; Meitinger et al., 2013; Oh et al., 2013), or through septin-binding proteins such as Bni5, which links septins to the myosin-II heavy chain Myo1 (Lee et al., 2002; Fang et al., 2010; Finnigan et al., 2015). During cytokinesis, the septin double rings were proposed to function as a diffusion barrier for proteins such as the exocyst component Sec3 and chitin synthase II Chs2 at the division site (Dobbelaere and Barral, 2004). But other studies have challenged this view by showing that Chs2 localizes efficiently to the division site in the absence of septin rings (Wloka et al., 2011). Regardless of the debate, septins are known to play essential roles in budding yeast cytokinesis. However, no physical interactions between septins and the exocyst have been reported, even in the genome wide interactome studies (Michaelis et al., 2023). Moreover, budding yeast septins also serve as scaffolds for the localization of hundreds of proteins at the bud neck including signaling proteins, bud site selection proteins, and chitin synthases (Longtine et al., 1996; DeMarini et al., 1997; Gladfelter et al., 2001; Longtine and Bi, 2003; Marquardt et al., 2019).

Unlike in budding yeast, septins are not essential in the fission yeast *Schizosaccharomyces pombe* and their roles in cytokinesis remain obscure (Longtine et al., 1996; Berlin et al., 2003; Tasto et al., 2003; Wu et al., 2010; Zheng et al., 2024). Fission yeast has seven septins, Spn1 to Spn7, with Spn1 to Spn4 expressing in vegetative cells and functioning at the division site (Longtine et al., 1996; Berlin et al., 2003; Tasto et al., 2003; An et al., 2004; Petit et al., 2005; Onishi et al., 2010; Wu et al., 2010). None of the Spn1-Spn4 is essential, but loss of some or all of them

causes a delay in cell separation, resulting in multi-septated phenotype (An et al., 2004). Spn1 and Spn4 are the more important components of the septin ring structure during cytokinesis (An et al., 2004). Septins accumulate to the division site shortly before the contractile ring constriction and form a single ring which quickly transitions into unconstricting double rings (Berlin et al., 2003; Tasto et al., 2003; Wu et al., 2003; Wu et al., 2010). It is only known that septin rings recruit the guanine nucleotide exchange factor Gef3 (Muñoz et al., 2014; Wang et al., 2015), the small GTPase Rho4 (Wang et al., 2015), and the glucanases Eng1 and Agn1 to the division site (Martin-Cuadrado et al., 2005). Thus, we know much less about fission yeast septins compared to those in budding yeast. It remains mysterious what the most conserved functions of septins are during evolution.

Previous studies have suggested that septins function in exocytosis (Hsu et al., 1998; Vega and Hsu, 2003; Martin-Cuadrado et al., 2005; Perez et al., 2015; Tokhtaeva et al., 2015). Fission yeast septins are proposed to work with the exocyst complex to regulate the secretion of glucanases at the appropriate location, but it was reported that septins and the exocyst are independent for localization (Martin-Cuadrado et al., 2005; Perez et al., 2015). The exocyst is a highly conserved, octameric complex (Sec3, Sec5, Sec6, Sec8, Sec10, Sec15, Exo70, and Exo84) in exocytosis (TerBush et al., 1996; Wang et al., 2002; Hsu et al., 2004; Heider and Munson, 2012; Liu and Guo, 2012). It functions in late stages of exocytosis by promoting the tethering and fusion of post-Golgi secretory vesicles to the plasma membrane (TerBush et al., 1996; Hsu et al., 2004; Liu et al., 2018). Although studies suggest that septins regulate the exocyst complex and a possible involvement of septins in targeting secretory vesicles to the exocytic sites (Hsu et al., 1998; Vega and Hsu, 2003; Li et al., 2007; Gupta et al., 2015), no direct interactions between septins and the exocyst subunits have been reported in budding yeast and other organisms.

Here we report septins regulate the exocyst localization and vesicle targeting in fission yeast via physical interactions. We find that the loss of septin rings alters the exocyst localization, with increased concentration to the center and reduced localization to the rim of the division plane. The initial recruitment of the exocyst is independent of septins, but the exocyst requires septin rings to maintain the rim localization during furrow ingression. Consistently, we found multivalent direct physical interactions between septins and the exocyst subunits. Loss of the exocyst ring leads to abnormal accumulation of secretory vesicles in septin mutants. As a result, the glucan synthase Bgs1 accumulates more to the center and the glucanase Eng1 is missing from the rim of the division plane, contributing to a thicker septum and a delayed cell separation in septin mutant cells. Our findings provide insights into the regulation of the exocyst localization and function on the plasma membrane by septins in other systems.

Results

Septin and the exocyst complex colocalize and are partially interdependent for localization at the division site

Both septins and the exocyst complex localize to the division site during cytokinesis (Longtine et al., 1996; Wang et al., 2002; An et al., 2004; Petit et al., 2005). To understand if and how they work together, we first examined the colocalization of the septin Spn1 and the exocyst subunit Sec3 in fission yeast. Spn1 is a key component in septin structures, and its loss leads to complete disruption of the septin rings from the division site (An et al., 2004). Sec3 is a spatial landmark for exocytosis in budding yeast (Finger et al., 1998; Boyd et al., 2004; Luo et al., 2014). The fission yeast Sec3 is an essential gene and crucial for exocyst localization (Kim et al., 2010; Bendezu et al., 2012; Jourdain et al., 2012). Spn1 and Sec3 colocalized at the division site as a single ring first, and later as double rings during septum formation (**Figure 1**, A and B). Sec3, but not Spn1, also concentrated at cell tips (**Figure 1C**). However, Sec3 arrived at the

division site 13.4 ± 2.2 min after spindle pole body (SPB) separation, about 10 min earlier than Spn1 that arrived at 23.6 ± 1.8 min (**Figure 1**, C and D). Time lapse movies of Exo70-tdTomato and Spn1-mEGFP confirmed that the exocyst appeared at the division site earlier than septins (Video 1). This suggests that the colocalization required for their proper function occurs at a specific stage during cytokinesis rather than a general regulation throughout the cell cycle.

Since septin and the exocyst colocalize at the division site and Sec3 arrives earlier, we tested whether septin localization depends on Sec3 and other exocyst subunits. In WT cells, Spn1 always formed ring structures at the rim of the division plane during septation (**Figure 1E**). In exocyst mutants *exo70*Δ and the temperature sensitive *sec3-913* and *sec8-1*, Spn1 localization was comparable to WT at permissive temperature (Figure supplement S1A). At restrictive temperature, although Spn1 localized as ring at the division site before septation, a fraction of Spn1 abnormally spread onto the division plane following furrow ingression in *sec3-913* and *sec8-1* mutants (**Figures 1E**, red boxes; and Figure supplement S1B, middle focal plane). As *exo70*Δ cells have no severe defects (Wang et al., 2003), the exocyst complex may not be as compromised as in *sec3-913* and *sec8-1* mutants. Only minor mislocalization of Spn1 was observed in *exo70*Δ cells even at 36°C (Figure supplement S1B). This localization pattern in exocyst mutants suggested a possible correlation between septins and the furrow ingression. Indeed, some Spn1 followed the contractile ring marked with Rng8 (Wang et al., 2014) as it constricted, spread onto the new plasma membrane, and concentrated at the center of the division plane while maintaining its localization at the rim (**Figure 1F**). We also examined Spn1 levels at the division site in cells with no visible septum, forming septum, and closed septum. Spn1 levels were comparable or higher in exocyst mutants compared to WT at both 25°C and 36°C (**Figures 1G** and Figure supplement S1, C and D). FRAP analyses of Spn1 showed no difference in its dynamics in WT and *sec3-913* cells at 36°C (**Figure 1H** and Figure supplement S1E). Collectively, despite some Spn1 mislocalizes to the center of the division plane in exocyst mutants, majority of Spn1 still localizes to the rim (**Figures 1E** and Figure supplement S1B). Thus, septins only partially depend on the exocyst for their localization.

Next, we examined the localization and levels of the exocyst complex (subunits Sec3, Exo70, and Sec8) in *spn1*Δ cells. In mitotic cells without a septum, the exocyst localized to the rim of the division plane in both WT and *spn1*Δ cells (**Figures 2A** and Figure supplement S1, F and G, yellow boxes). During septation, however, the exocyst spread across the division plane as a disk in *spn1*Δ cells while it remained at the rim in WT cells (**Figures 2A** and Figure supplement S1, F and G, red boxes). The levels of Sec3, Exo70, and Sec8 at the division site in *spn1*Δ cells were not significantly different from WT before septation (**Figures 2B** and Figure supplement S1H). During and after septum formation, the levels of all three exocyst components were significantly reduced at the division site (except Exo70 in cells with forming septum) and almost absent at the rim in *spn1*Δ cells (**Figures 2A** and Figure supplement S1H). These results were confirmed in cells expressed Sec8-GFP and myosin light chain Rlc1 as a contractile ring marker (**Figure 2**, D and E). However, the dynamics of Sec3 at the division site was not affected in *spn1*Δ cells (**Figures 2C** and Figure supplement S1I). The exocyst was much more dynamic than septins at the division site (**Figures 1H** and **2C**), which was confirmed by high temporal resolution imaging of Exo70 (Video 2 and 3). Together, loss of septins results in exocyst mislocalization and its decreased levels, especially at the rim of the division plane during septum formation, suggesting that septins play an important role in regulating the exocyst localization at the division site.

Collectively, our data suggest that septins and the exocyst complex are interdependent for localization at the division site during and after the contractile ring constriction, with the septin rings being more important for the exocyst localization. Thus, we conclude that the initial recruitment of the exocyst to the division site does not depend on septins, but its rim localization and maintenance during late cytokinesis require the septin rings.

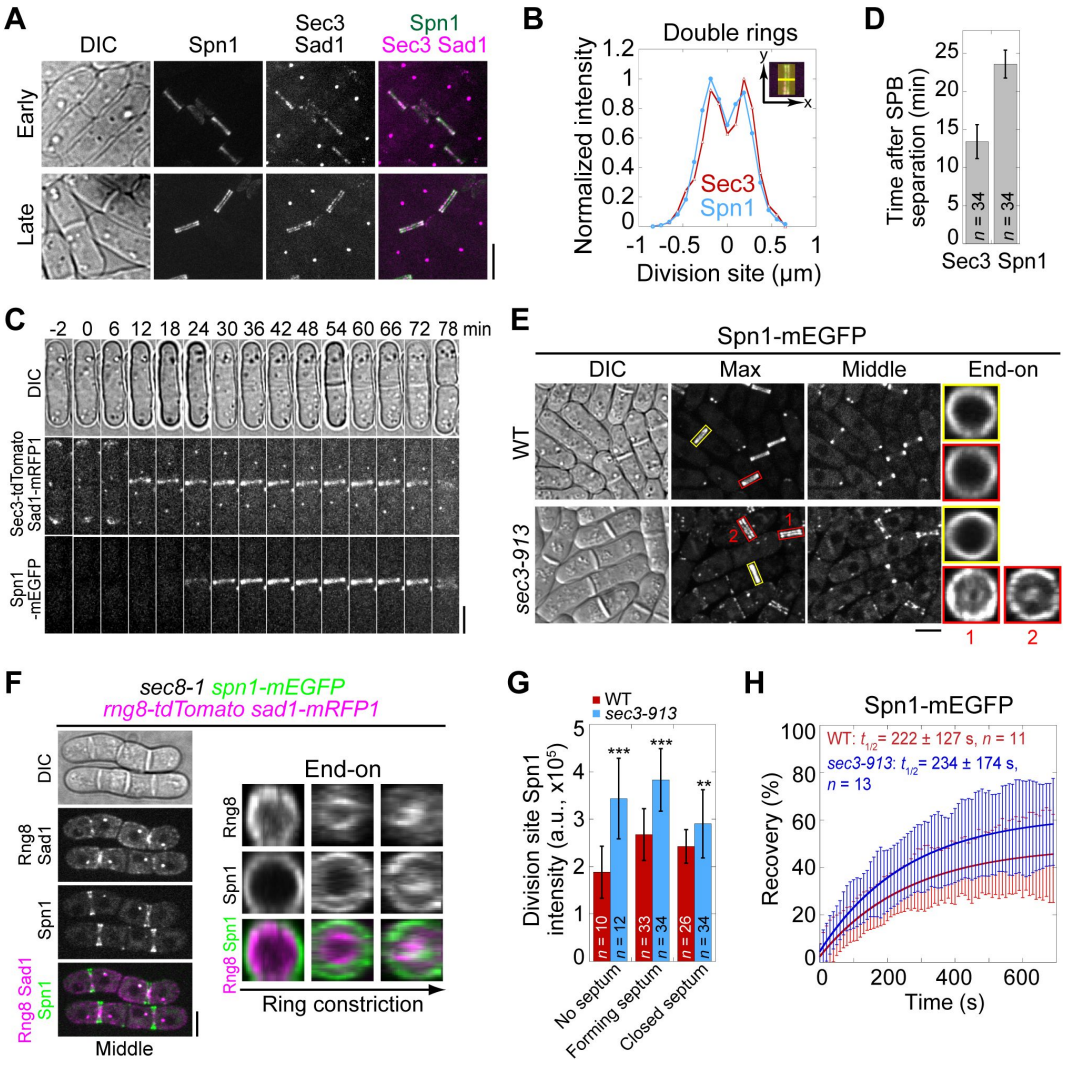

Figure 1.

Septins and the exocyst colocalize at the division site and septins partially depend on the exocyst for localization. (A)

Co-localization of Spn1-mEGFP and Sec3-tdTomato at the division site in cells without (early) and with (late) septa. Sad1-mRFP1 marks the spindle pole body (SPB). **(B)** Line scans showing Spn1 and Sec3 intensities across the division site along the cell long axis in septated cells as in (A). **(C)** Time course and **(D)** quantification (in minutes) of Sec3 and Spn1 localizations and appearance timing (D) at the division site. SPB separation is defined as time 0. **(E)** Localization of Spn1 (Max intensity projection, Middle focal plane, and End-on view of the division site) in WT and *sec3-913* cells grown at 36°C for 4 h. Yellow boxes, cells without septa; Red boxes, cells with septa. **(F)** Localization of Spn1 and the contractile-ring marker Rng8 in *sec8-1* cells grown at 36°C for 4 h. **(G)** Spn1 intensities at the division site in WT and *sec3-913* cells grown at 36°C for 4 h. Cells were grouped into no septum, forming septum, and closed septum stages. **, P < 0.01; ***, P < 0.001. **(H)** FRAP analyses (photobleached at time 0) of Spn1 at the division site in WT and *sec3-913* cells grown at 36°C for 4 h. Mean ± SD. Bars, 5 μm.

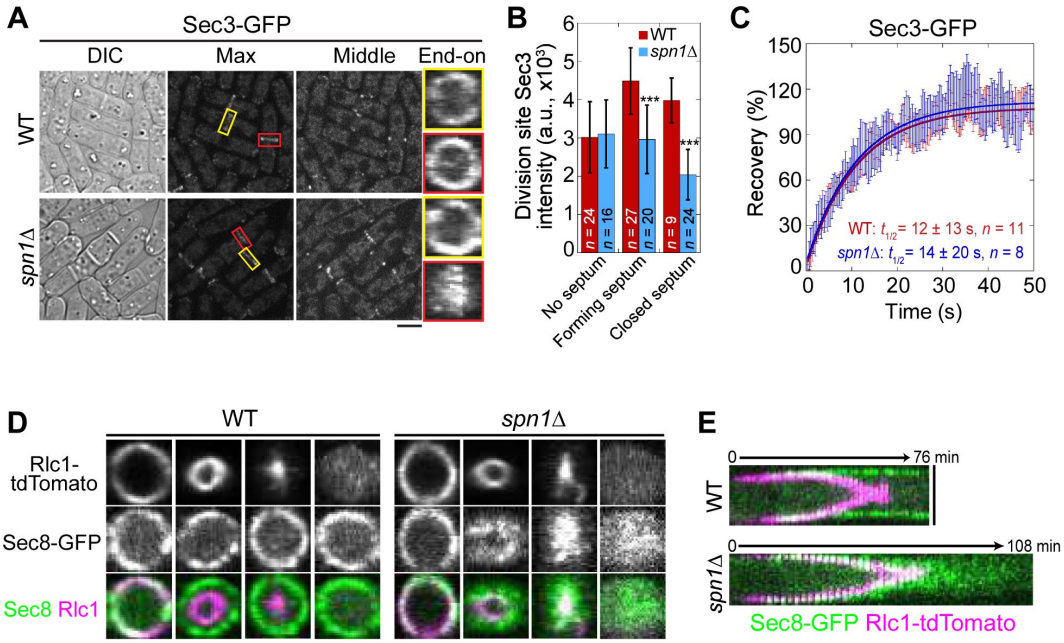

Figure 2.

Septin rings recruit or anchor the exocyst complex to the rim of the division plane during late stage of cytokinesis. (A)

Localization of Sec3 at the division site in WT and *spn1*Δ cells. Yellow boxes, cells without a septum; Red boxes, cells with a closed septum. **(B)** Sec3 intensity at the division site in WT and *spn1*Δ cells. ***, P < 0.001. **(C)** FRAP analyses of Sec3 at the division site in WT and *spn1*Δ cells. Mean ± SEM. **(D** and **E)** End-on views (D) and kymographs (E) of Sec8 and the contractile ring marker Rlc1 at the division site in WT and *spn1*Δ cells. Bars, 5 µm.

Septins regulate the exocyst localization through direct physical interactions

Septins have been shown to play a role in the Rho GEF Gef3-Rho4 GTPase pathway to regulate the exocytosis of glucanases Eng1 and Agn1 for proper cell separation (Perez et al., 2015; Wang et al., 2015). Septins are essential for Gef3 localization to the division site (Wang et al., 2015). In *spn1*Δ cells, Gef3 localization on the plasma membrane is abolished, and Rho4 localization in cells with a closed septum was significantly reduced (Wang et al., 2015). Since Rho4 can interact with both the exocyst complex and septins (Perez et al., 2015), we tested whether the altered exocyst localization pattern that we observed in septin mutants was through Gef3 and Rho4. Although partially mislocalized to the center of the division plane, majority of Sec3 still localized as a ring at the rim of division plane in *rho4*Δ, *gef3*Δ, and *rho4*Δ *gef3*Δ cells (Figure supplement S2A). Moreover, Spn1 ring localization was not affected in *rho4*Δ *gef3*Δ cells (Figure supplement S2B). Thus, the different localization patterns of the exocyst in *spn1*Δ and *rho4*Δ *gef3*Δ cells suggest that septins can regulate exocyst localization independent of Gef3 and Rho4.

To test the hypothesis that septins regulate the localization of the exocyst directly, we examined the physical interactions between septins and the exocyst subunits. Sec3 and Exo70 are the most important subunits for the targeting of the octameric exocyst to the plasma membrane (Boyd et al., 2004; He et al., 2007; Bendezu et al., 2012; Luo et al., 2014; Yue et al., 2017; Liu et al., 2018; Synek et al., 2021), and Spn1 and Spn4 are essential for septin localization and functions (An et al., 2004). Therefore, we first tested the interactions between Spn1-Sec3, Spn1-Exo70, Spn4-Sec3, and Spn4-Exo70 using co-immunoprecipitation of cell extracts from fission yeast. Surprisingly, no physical interactions were detected among the four proteins.

Then we utilized AlphaFold2_advanced ColabFold algorithm (Jumper et al., 2021; Mirdita et al., 2022), whose highly accurate predictions of protein structures have revolutionized structural biology, to predict the physical interactions between all 32 combinations of the four septins and eight exocyst subunits. For the modeling, the complete sequences of each subunit of septins and exocyst complex were used except Sec8. Sec8 subunit was analyzed in two fragments with overlapping sequence due to the 1,400 amino acids input sequence limitation of AlphaFold2_advanced. Representative models generated are shown (**Figures 3** and Figure supplement S3). Predicted interacting interface residues defined as amino acids of two possible binding partners with distance ≤4 Å were calculated from the rank 1 predicted model (Yin and Pierce, 2023). Moreover, the contacts between interface residues having pLDDT score >50 were calculated. Based on the above analyses, we predicted the following top six interactions between the septin and exocyst subunits: Spn2 and Sec15 (**Figure 3**), Sec15 and Spn1, Sec6 and Spn1, Spn2 and Sec5, Spn4 and Sec15, and Spn4 and Sec3 (Figure supplement S3).

Next, we used reciprocal Co-IP assays of fission yeast extracts to confirm the predicted interactions between septin and exocyst subunits by AlphaFold2_advanced ColabFold. Out of the six predicted interactions, we found five of them were positive in Co-IP. We found that Spn2 physically interacted with Sec5 and Sec15, Spn1 with Sec15 and Sec6, and Spn4 with Sec15 (**Figures 4** and Figure supplement S4). Sec15 interacts with three septins Spn1, Spn2, and Spn4, which was stronger than other combinations. We also utilized yeast two-hybrid assays to test whether these five-pair interactions are direct (**Figure 4**, E and F). X-gal overlay assay (insets) and quantification of β-galactosidase using ONPG confirmed that Sec15 directly interacted with Spn1, Spn2, and Spn4 (**Figure 4E**); and Sec6 interacted with Spn1 and its C-terminal fragment (Spn1[300-469]) that contains the coiled-coil motif (**Figure 4F**). The Spn2-Sec5 interaction could not be tested due to very high level of autoactivation of Sec5. Thus, we conclude that septins physically and directly interact with the exocyst complex in fission yeast via multivalent interactions.

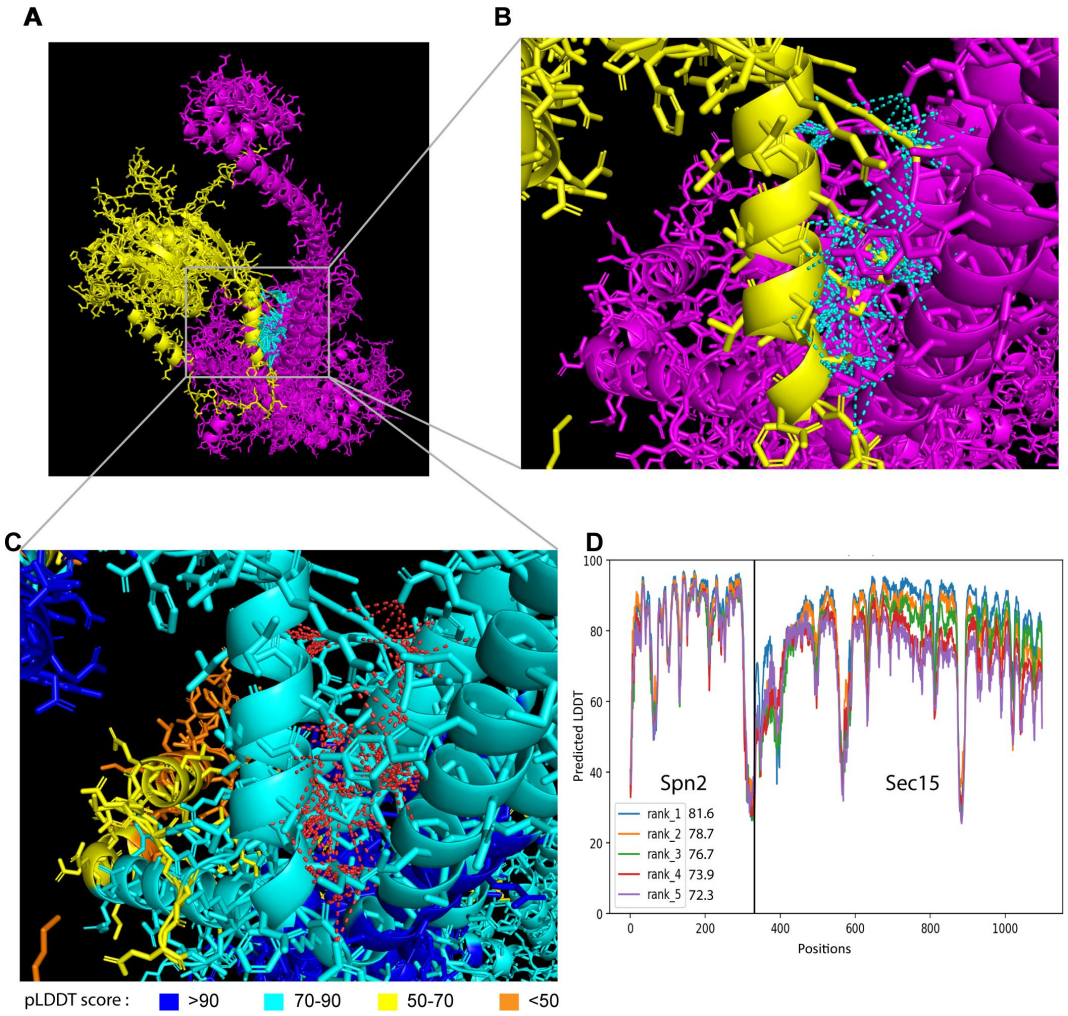

Figure 3.

The 3D structural model of predicted interactions between Spn2 and Sec15 generated by AlphaFold. (A)

AlphaFold2_advanced predicted interaction between Spn2 and Sec15 in rank 1 model with pLDDT score of 81.6. **(B, C)** Inset of enlarged view of the predicted interactions. Spn2 is colored in yellow and Sec15 in magenta, contacts between interface residues with distance <4 Å are colored in cyan in (A, B). Residues in (C) are colored corresponding to their pLDDT scores as indicated in the legends below, contacts between interface residues with distance < 4 Å are colored in red. **(D)** Residue position scores of five predicted models for Spn2 and Sec15 interactions ranked according to pLDDT scores.

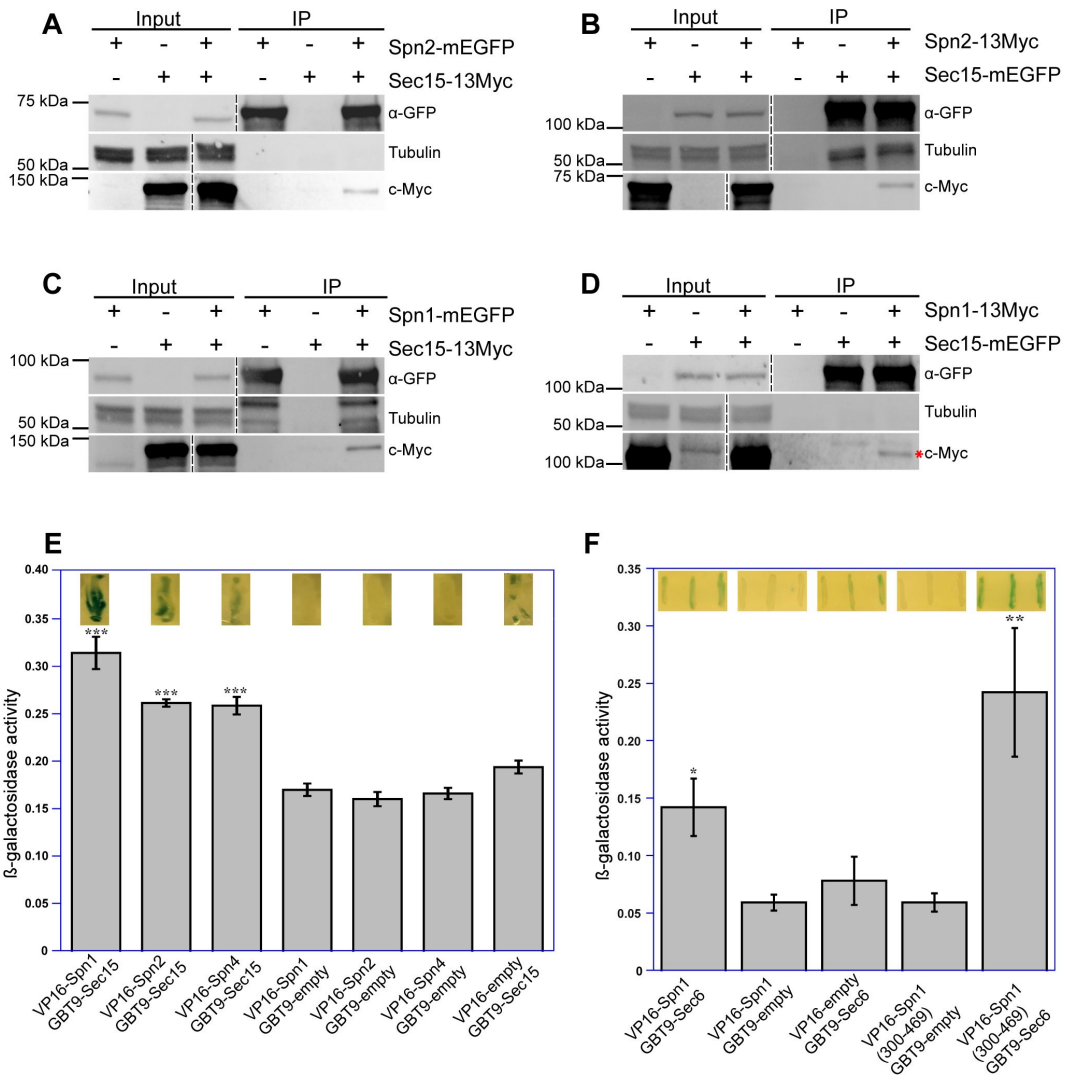

Figure 4.

Septins and the exocyst interact physically and directly.

Reciprocal coimmunoprecipitation of Sec15 with Spn2 **(A** and **B)** and Spn1 **(C** and **D)**. Septin or exocyst subunits tagged with mEGFP or 13Myc were immunoprecipitated using antibodies against GFP from cell lysates, separated on SDS-PAGE, and incubated with appropriate antibodies. Tagged proteins were detected on iBright Imager. Tubulin was used as a loading control. Asterisk (*) in D marks Spn1-13Myc. The vertical dashed lines mark the positions of protein ladders that was excised out. (**E** and **F**) Septins and the exocyst subunits interact directly revealed by the yeast two-hybrid assays. X-gal overlay results (insets on the top of the columns) and quantification of β-galactosidase activities using ONPG showing interactions between (E) Sec15 with Spn1, Spn2, and Spn4; and (F) Sec6 with Spn1 and its coil-coil motif Spn1(300-469). Data is shown in Mean ± SD, n = 3 (in E) or 4 (in F). ***p ≤ 0.0001, **p ≤ 0.001, *p ≤ 0.01 compared with their respective controls in one-way ANOVA with Tukey's post hoc test.

Septins are involved in concentrating Sec15 and Sec5 at the rim of the division site especially at the late-stage cytokinesis

We reasoned that septins localize the exocyst at the division site via their multivalent interactions with the exocyst subunits Sec15, Sec5, and Sec6. Weakened interactions between septins and the exocyst in the absence of a certain septin subunit could lead to mislocalization of the exocyst complex. Indeed, similar to the results presented in **Figures 1**, 2, and Figure supplement S2 with other exocyst subunits, the deletion of *spn1* or *spn4* led to mislocalization of Sec15 on the division plane in ~75% of cells with a septum while Sec15 in ~90% of WT cells localized as rings at the rim of the division plane in septating cells (**Figure 5**, A and B). Results from time-lapse microscopy of *spn1Δ* or *spn4Δ* cells were consistent with these findings. Sec15 was first recruited to division site as rings and then spread to whole division plane before signal disappearance, leading to some multiseptated cells (Videos 4-6).

Although septin filaments have four subunits in vegetative cells (An et al., 2004), Spn2 is less important than Spn1 and Spn4 for septin functions and *spn2Δ* has a much weaker phenotype in septation than *spn1Δ* or *spn4Δ* (An et al., 2004; Wu et al., 2010; Zheng et al., 2018). Consistently, in *spn2Δ* cells, Sec15 and Sec5 localized normally at the division site before septation (**Figure 5**, A and C). Both Sec15 and Sec5 spread to the whole division plane in ~50% of *spn2Δ* cells with obvious septa observed in the DIC channel (**Figure 5**, A-D). Unlike in *spn1Δ* or *spn4Δ* cells, a fraction of Sec15 and Sec5 can still localize to the rim in *spn2Δ* cells. Collectively, these data support that Spn1, Spn2, and Spn4 are important for restricting the exocyst to the rim of the division plane during cytokinesis through direct physical interactions.

Septin mutants affect the sites of secretory vesicle tethering and cargo delivery at the division plane

Septin and exocyst mutations showed no or very mild synthetic genetic interactions (**Tables 1** and **2**), suggesting that septins and the exocyst complex function in the same pathway to regulate cytokinesis and septation. Surprisingly, they have different genetic interactions with the transport particle protein-II (TRAPP-II) mutants (**Tables 1** and **2**). The exocyst mutant *sec8-1* is synthetic lethal with *trs120-M1* and has severe synthetic cytokinesis defects with *trs120-ts1* due to the overlapping function of the exocyst and TRAPP-II in exocytosis during fission yeast cytokinesis (Wang et al., 2016). However, *spn1*Δ *trs120-M1* and *spn1*Δ *trs120-ts1* double mutants were viable with no obvious synthetic interactions (**Tables 1** and **2**). Thus, septins and the exocyst also function in different genetic pathways in fission yeast.

The exocyst complex is the major tether of secretory vesicles at the plasma membrane (TerBush and Novick, 1995; TerBush et al., 1996; Wang et al., 2002; Luo et al., 2014). So, we tested whether exocyst mislocalization in septin mutants compromises the targeting of secretory vesicles and their cargos. We first performed electron microscopy to examine if secretory vesicles are accumulated at the division site in *spn1*Δ cells (**Figure 6A**). During septum formation, 7– and 2-fold more secretory vesicles accumulated at the division site in *sec8-1* and *spn1*Δ cells, respectively, compared to WT (**Figure 6**, A and B). However, in cells with a closed septum, the number of secretory vesicles adjacent to the division site were not significantly different between WT and *spn1*Δ cells (**Figure 6B**). Consistently, secretory vesicle markers Rab11 GTPase Ypt3 and v-SNARE Syb1 accumulated more in the center of the division plane but diminished from the rim in *spn1*Δ cells (**Figure 6**, C and D). The accumulation of the secretory vesicles at the division plane and their mistargeting are consistent with exocyst mislocalization in *spn1*Δ cells.

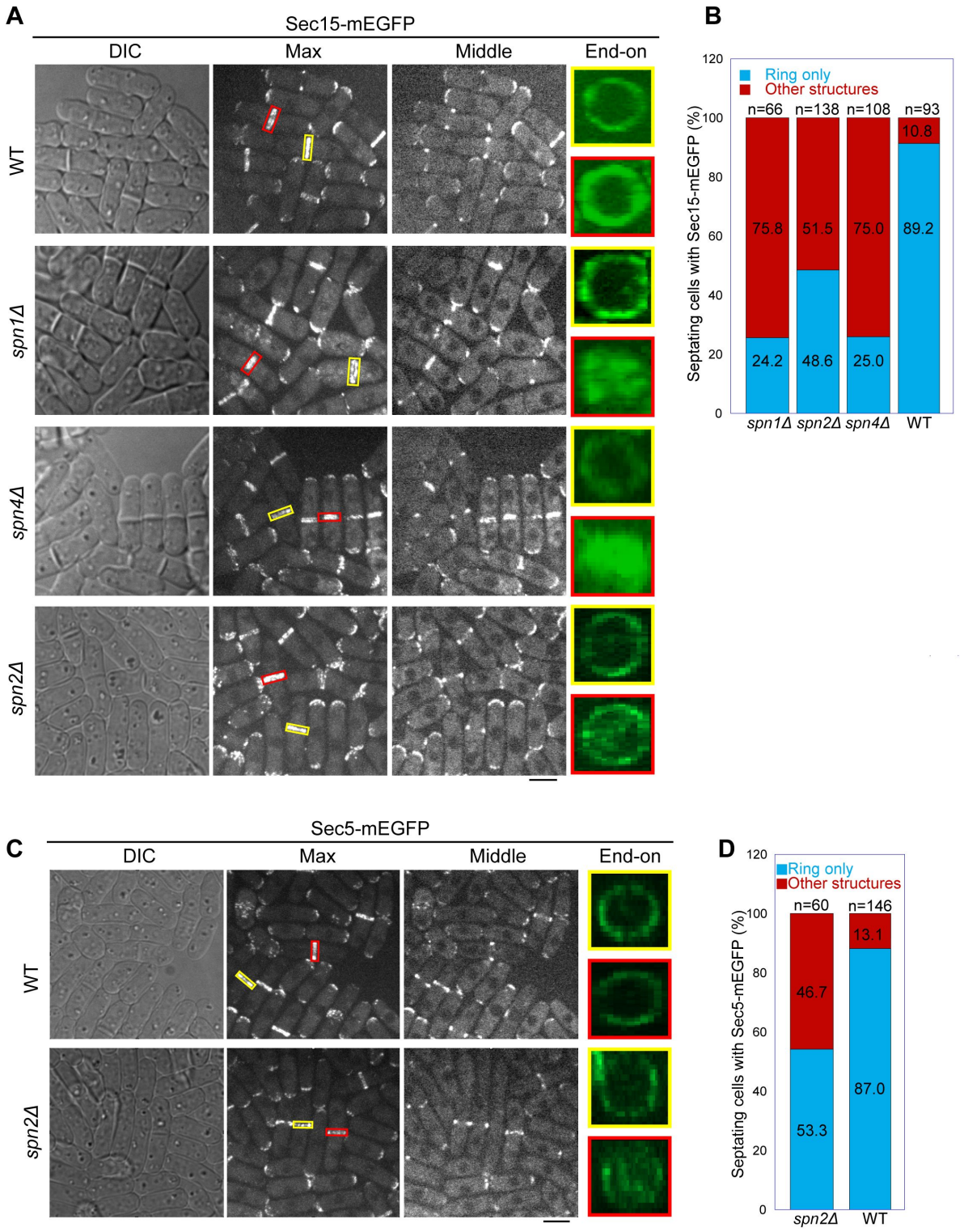

Figure 5.

Localization patterns of both Sec15 and Sec5 at the division site depend on septins.

Localization of **(A, B)** Sec15 and **(C, D)** Sec5 at the division site in WT and septin mutant cells. Yellow boxes, cells without a septum; Red boxes, cells with a closed septum in (A, C). (B, D) Quantification of cells with intact and mislocalized Sec15 (B) and Sec5 (D) signals in WT and septin mutant cells with obvious septa. Scale bars, 5 μm.

Parent 1	Parent 2	Viable double mutants (%) at 25°C	Total number of tetrads	Genetic interaction at 25°C[a]
spn1Δ	*sec3-916*	78	14	+
spn1Δ	*sec3-913*	100	13	-
spn1Δ	*sec8-1*	100	12	-
spn1Δ	*exo70Δ*	100	14	-
spn1Δ	*trs120-M1*	100	27	-
spn1Δ	*trs120-ts1*	95	18	-
spn2Δ	*sec3-916*	83	10	+
spn2Δ	*sec3-913*	100	10	-
spn3Δ	*sec3-916*	100	12	+
spn3Δ	*sec3-913*	75	11	-
spn4Δ	*sec3-916*	80	10	+
spn4Δ	*sec3-913*	100	14	-
spn4Δ	*sec8-1*	100	11	-

[a]Cells were freshly grown on YE5S and YE5S plus Phloxin B (PB, which accumulates in dead cells) plates before checking the morphology under DIC. The severity of cytokinesis defects compared with the parents was classified as follows: -, no additive cytokinesis defects; +, mild synthetic interaction.

Table 1.

Genetic interactions between septin and exocyst mutations

Mutations	25°C	30°C	32°C	36°C
sec3-916	+++[b]	++[c]	+[d]	-[e]
sec3-913	+++	+++	++	-
sec8-1	+++	++	+	-
spn1Δ	++	++	++	++
spn1Δ sec3-916	++	+	-	-
spn1Δ sec3-913	++	++	++	-
spn1Δ sec8-1	++	++	+	-
exo70Δ	+++	+++	++	-
spn1Δ exo70Δ	++	++	++	-
trs120-M1	++	-	-	-
spn1Δ trs120-M1	++	-	-	-
trs120-ts1	+++	+++	+	-
spn1Δ trs120-ts1	++	++	+	-
spn2Δ	+++	+++	+++	+++
spn2Δ sec3-916	++	+	+	-
spn2Δ sec3-913	+++	++	+	-
spn3Δ	+++	+++	+++	+++
spn3Δ sec3-916	++	++	+	-
spn3Δ sec3-913	+++	++	++	-
spn4Δ	++	++	++	++
spn4Δ sec3-916	++	+	-	-
spn4Δ sec3-913	++	++	++	-
spn4Δ sec8-1	++	++	++	-

[a]Colonies growth and color on YE5S + phloxin B plates at various temperatures.
[b]+++, comparable to wt.
[c]++, some cell lysis or cytokinesis defects.
[d]+, severe cytokinesis defects with reduced growth.
[e]-, inviable.

Table 2

Genetic interactions between septin and exocyst mutations

.[a]

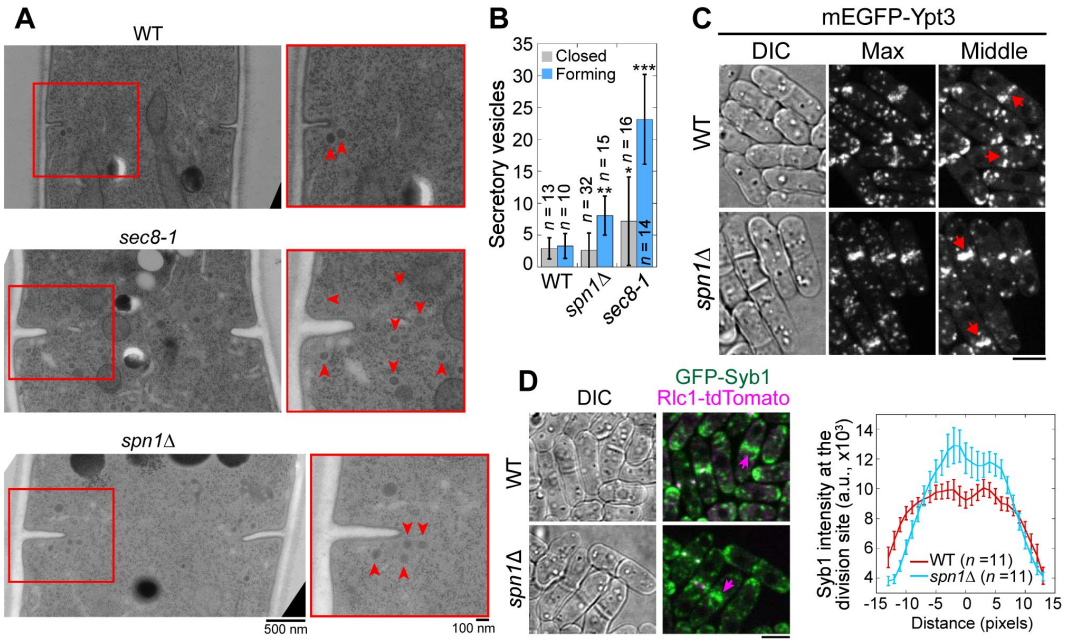

Figure 6.

Septins are important for proper localization and distribution of secretory vesicles.

(**A** and **B**) EM thin-section images (A) and quantifications of secretory vesicles (B) in WT, *sec8-1*, and *spn1*Δ cells with forming or closed septa. Cells were grown at 36°C for 4 h. Red boxes indicate the enlarged regions on the right. Arrowheads mark secretory vesicles. *, P < 0.05; **, P < 0.001; ***, P < 0.0001 compared to WT. **(C** and **D)** Localizations of Rab11 GTPase Ypt3 (C) and v-SNARE Syb1 and Rlc1 (D) in WT and *spn1*Δ cells. Arrows mark examples of cells with closed septa. Syb1 intensities at the division site (D, right) from line scans at the middle focal plane of cells with full septa. Bars, 500 nm (A, left), 100 nm (A, right), and 5 μm (C and D).

We next examined the distribution of two secretory vesicle cargos, β-glucan synthase Bgs1 and β-glucanase Eng1, which were delivered to the division site by the secretory vesicles during cytokinesis (Liu et al., 1999; Baladrón et al., 2002; Cortes et al., 2002; Martin-Cuadrado et al., 2003). More Bgs1 localized in the center of the division plane in *spn1*Δ cells compared to WT (**Figure 7A**). *spn1*Δ and *sec8-1* cells also had a much thicker septum compared to WT cells (**Figure 7B**). Another cargo of secretory vesicles, Eng1, spread across the division plane as a disk with localization clearly missing at the rim in *spn1*Δ cells (**Figure 7C**). Lack of glucanase Eng1 at the rim could contribute to the delayed cell separation in *spn1*Δ cells since the junctions between septum and the cell wall cannot be efficiently digested, consistent with earlier studies (Baladrón et al., 2002; Martin-Cuadrado et al., 2003). Our studies on Bgs1 and Eng1 indicate an increase of vesicle tethering in the center and a loss at the rim of the division plane without septins.

Collectively, our data indicate that septins play important roles in maintaining the proper localization of the exocyst complex on the plasma membrane. This regulation on the exocyst occurs specifically during late stages of cytokinesis in fission yeast. Loss of septins results in spreading of the exocyst across the division plane with significant reduction at the rim, which leads to the accumulation of secretory vesicles and mistargeting of downstream cargos.

Discussion

In this study, we reveal how septins and the exocyst complex physically interact to regulate exocytosis and ensure proper targeting of vesicle cargos to the plasma membrane.

Septins are important for proper membrane targeting of the exocyst complex to ensure successful cytokinesis

Septins are essential for cytokinesis and other cellular processes in budding yeast and many other organisms (Neufeld and Rubin, 1994; Longtine et al., 1996; Kinoshita et al., 1997; Gladfelter et al., 2001; Russell and Hall, 2005; Oh and Bi, 2011). However, the nature of their functions is only partially understood. It has been a mystery why the phenotypes of septin mutants are so mild in fission yeast ever since their discoveries in the early 1990s, yet their sequences and structures are evolutionarily conserved across species (An et al., 2004; Zheng et al., 2018; Zheng et al., 2024). In human, dysregulation of septins or exocyst complex leads to severe disorders including neurological diseases and cancers (Russell and Hall, 2005; Martin-Urdiroz et al., 2016; Halim et al., 2023; Werner and Yadav, 2023). Thus, it is critical to identify the functional links between septins and exocyst complex for better understanding and treatment of related diseases. In this study, we investigated the spatial regulation of the exocyst complex and roles of septins during cytokinesis in the fission yeast model system. Without septin rings, the exocyst complex, which specifies for the sites for vesicle fusion on the plasma membrane, cannot maintain its localization at the rim of the division plane. Instead, the exocyst complex follows actomyosin contractile ring constriction and spreads across the whole division plane. This localization dependence on septin rings occurs in a specific spatiotemporal manner at the division site during furrow ingression stage of cytokinesis. Although loss of septins does not affect the dynamics of the exocyst, the targeting sites of secretory vesicles and their cargos are altered, which contributes to a thicker septum and a delayed cell separation. Thus, fission yeast septins function in exocytosis through maintaining proper docking sites of the exocyst complex and secretory vesicles at the division site.

Fission yeast septins regulate the exocyst in specific temporal and spatial manners. They only regulate the localization of the exocyst during late stages of cytokinesis and are not responsible for its targeting to the cell tips during interphase or initial recruitment to the division site during early cytokinesis. Disruption of the contractile ring affects the localization of the exocyst to the division site (Wang et al., 2002; Dobbelaere and Barral, 2004). This suggests that the exocyst likely

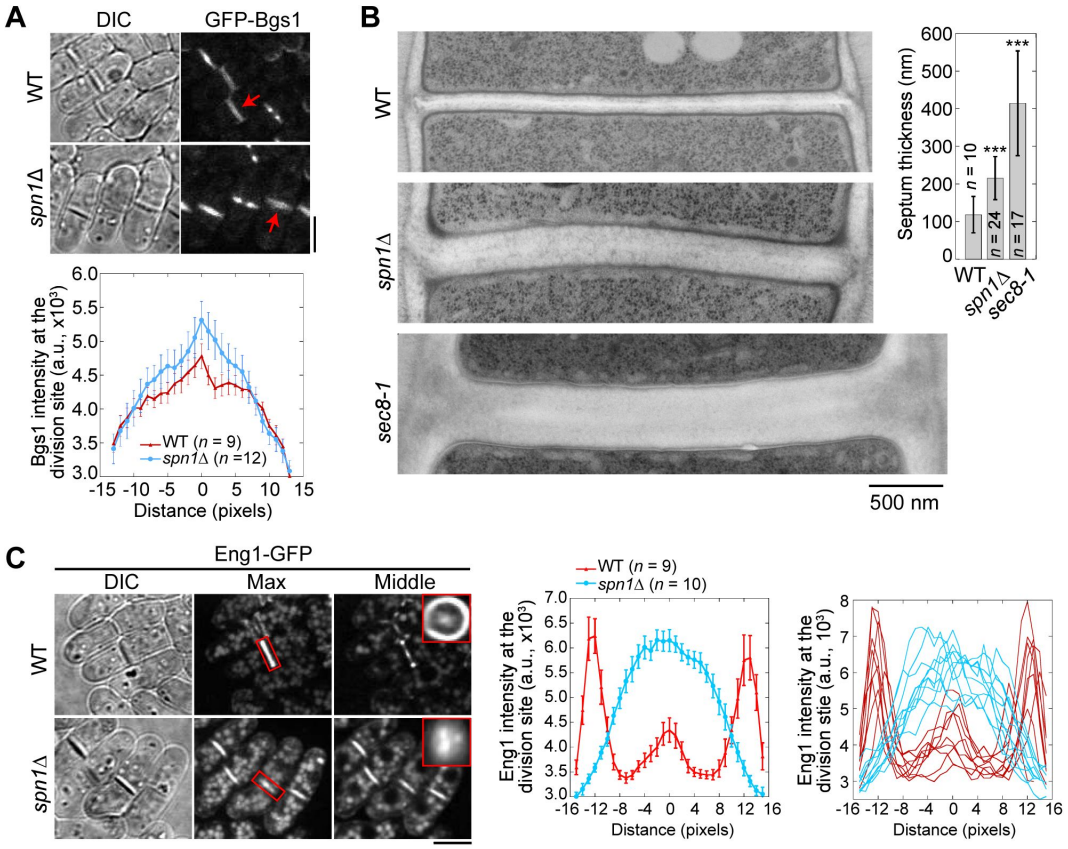

Figure 7.

Septins are important for localization and distribution of secretory cargos Bgs1 and Eng1. (A)

Localization (top) and intensity (bottom) of glucan synthase Bgs1 in WT and *spn1*Δ cells. Arrows mark examples of cells with a closed septum. Bgs1 intensities from line scans across the division site at the middle focal plane were compared in cells with closed septa. **(B)** EM thin-section images (left) and septum thickness (right) of WT, *spn1*Δ, and *sec8-1* cells with closed septa. Cells were grown at 36°C for 4 h. ***, P < 0.0001 compared to WT. **(C)** Localization (left) and intensity (middle and right) of Eng1-GFP in WT and *spn1*Δ cells. The end-on views of Eng1 at the division site in cells with closed septa are shown as the insets. Eng1 intensities (Middle, mean intensities and Right, individual cells) are from line scans at the middle focal plane. Bars, 5 µm (A and C) and 500 nm (B).

depends on the contractile ring for initial recruitment to the division site. However, this is not a universal mechanism. Although budding yeast Sec8 localization depends on the actomyosin ring, Sec3 localization is independent of actin cytoskeleton (Finger et al., 1998). The subcellular localization of the exocyst complex in rat brain cells is affected by microtubule-disrupting drugs, but not actin-disrupting drugs (Vega and Hsu, 2003). Thus, how the exocyst is initially recruited to the division site remains to be studied. Since fission yeast exocyst clearly depends on septins for proper localization during late stages of cytokinesis, its localization dependence must transition to septins from the contractile ring at some point before the onset of the contractile ring constriction. So, it will be of great interest to examine how this transition occurs. Although septins may act as either scaffolds or diffusion barriers for Sec3 in budding yeast, Sec3 localizes between the split septin rings during cytokinesis (Dobbelaere and Barral, 2004). However, in mammalian neurons, the exocyst subunits Sec6 and Sec8 colocalize with the septin SEPT7/CDC10 (Hsu et al., 1998). Thus, the colocalized septins and the exocyst in fission yeast may provide more insights in mammalian cells for understanding the molecular mechanisms of their interactions.

Examples of localization dependence between septins and the exocyst have been reported in other systems. The most prominent cases come from fungal pathogens (Eisermann et al., 2023). *Magnaporthe oryzae* infects plants through a specialized infection cell called appressorium, which breaches through the cuticle of the leaf to allow entry into plant tissues (Dagdas et al., 2012; Gupta et al., 2015; Zhang et al., 2021). The exocyst assembles in appressorium at the point of plant infection in a septin-dependent manner. Septin deletion causes mislocalization of the key component for the exocyst assembly, Sec6, at the appressorium pore (Gupta et al., 2015). Similarly, the root-infecting phytopathogenic fungus *Verticillium dahliae* also assembles the exocyst at the penetration peg of the hyphopodium in a septin-dependent manner (Zhou et al., 2017). The absence of septin VdSep5 impairs the delivery of secretory proteins to the penetration interface (Zhou et al., 2017). Another example is *Candida albicans* septins, which localize at the hyphal tips where tip growth occurs with active exocytosis in this human opportunistic pathogen (Li et al., 2007). Deletion of septin *CDC10* or *CDC11* causes mislocalization of the exocyst marked by Sec3 (Li et al., 2007). Thus, one of the conserved roles of septins is to regulate the proper membrane targeting of the exocyst complex to the plasma membrane and to ensure spatiotemporal fidelity of vesicle tethering and fusion. However, how septins and the exocyst physically interact had not been systematically investigated. Our current study will provide insights on how fungal pathogens infect their hosts.

The exocyst complex docks on septins on the plasma membrane through multivalent physical interactions

Despite the relationships between septins and exocyst mentioned above, whether and how they physically interact with each other remain obscure. In budding yeast, the exocyst subunits have been shown to interact physically with a number of proteins, including Sec15 with Rab GTPase Sec4 and type V myosin Myo2; and Sec6 with v-SNARE protein Snc2, t-SNARE protein Sec9, and Sec1/Munc18 family protein Sec1 (Guo et al., 1999; Sivaram et al., 2005; Jin et al., 2011; Shen et al., 2013; Lepore et al., 2016). Evidence indicates that the septin dynamics is essential for exocytosis, but no direct interaction has been detected yet between septins and the exocyst (Tokhtaeva et al., 2015). Recently, Michaelis and colleges have mapped *S. cerevisiae* protein interactome and found no interactions between septins and exocyst in pull down experiments (Michaelis et al., 2023).

However, several interactions between septins and the exocyst have been identified by Co-IPs to support the role of septins in the regulation of the exocyst localization in other cell types (Hsu et al., 1998; Beites et al., 1999; Vega and Hsu, 2003; Li et al., 2007; Gupta et al., 2015). In rat brain lysates, the septins SEPT2, 4, 6 and 7 have been shown to associate with exocyst complex containing Sec6/8 (Hsu et al., 1998). Sec6 is found to be colocalized with SEPT7 on synapse assembly sites in isolated neurons where active membrane remodeling is required (Hsu et al.,

1998). From rat brain cells, exocyst subunits Sec8 and Exo70 along with tubulin co-immunoprecipitated with septin Nedd5 (Vega and Hsu, 2003). During hyphal development in *C. albicans*, association of Sec3 and Sec5 was detected by co-immunoprecipitation with Cdc3 (Li et al., 2007). In *M. oryzae,* mislocalization of Sec6 was reported with deletion of septin Sep3. This was supported by pull down and mass spectrometry data where Sep4 and Sep5 were pulled down by Exo84 while Sep3 by Sec6 (Gupta et al., 2015). Here we have presented the most comprehensive studies on explaining importance of septins to regulate exocytosis by direct physical interactions with the exocyst complex in fission yeast.

In our study, we systematically investigated all the potential pairwise interactions between septin and exocyst subunits using AlphFold2 predictions. We experimentally confirmed five out of the six predicted interactions by co-IPs: Spn1-Sec15, Spn1-Sec6, Spn2-Sec15, Spn2-Sec5, and Spn4-Sec15 and validated four of them by yeast two-hybrid assays (except Spn2-Sec5 due to high levels of Sec15 autoactivation). These multivalent interactions are able to ensure that the exocyst tethers secretory vesicles on the plasma membrane with high temporal and spatial fidelity even individual interaction may not be very strong. Interfaces of exocyst subunits Sec15, Sec6, and Sec5 are known to be available in the exocyst complex to interact with many proteins as mentioned above in budding yeast and in other systems for different cellular functions (Sjölinder et al., 2002; Fukai et al., 2003; Zhang et al., 2004; Feng et al., 2012; Du et al., 2015; Guo et al., 2016; Yang et al., 2022). The interactions between septins and the exocyst that we identified in fission yeast will provide important insights into the mechanisms of exocyst regulations by septins. During evolution, fission yeast may have lost many but these most conserved aspects of septin functions including septin-exocyst interactions.

It is known that the octameric exocyst complex consist of two subcomplexes (Heider et al., 2016; Ahmed et al., 2018; Lepore et al., 2018; Mei and Guo, 2018; Mei et al., 2018; Ganesan et al., 2020). Subcomplex 1 consist of Sec3, Sec5, Sec6, and Sec8 while subcomplex 2 consist of Sec10, Sec15, Exo70, and Exo84. In our study, we found that septins can interact with both of the exocyst subcomplexes with multivalent interactions by Alphafold predictions, reciprocal Co-IPs and yeast two-hybrid assays. Future studies are needed to map out the residues involved in the interactions. The predicted interacting residues from AlphaFold are too numerous and have to be refined. Preliminary examinations suggested that many of the predicted conserved residues on Sec15 and Sec5 are accessible for interactions with other proteins based on the structure of budding yeast exocyst (Lepore et al., 2018; Mei et al., 2018). In addition, tests are needed to figure out if posttranslational modifications are necessary for the interactions between septins and the exocyst. Because the colocalization of septins and the exocyst required for their proper function occurs at a specific stage during cytokinesis rather than a general regulation throughout the cell cycle, septin filament formation and posttranslational modifications of the involved proteins may be required, which make it challenging to tease out the interactions in vitro (Dobbelaere et al., 2003; Hernández-Rodríguez and Momany, 2012; Ren and Guo, 2012; Tay et al., 2019; Sharma and Menon, 2023; Werner and Yadav, 2023). Moreover, we cannot rule out that RhoA GTPase and PI(4,5)P2 are involved in septin-exocyst interactions as both has been reported to interact with septins and/or the exocyst in other cell types (Guo et al., 2001; He et al., 2007; Bertin et al., 2010; Bendezu and Martin, 2011; Perez et al., 2015; Carim and Hickson, 2023; Safavian et al., 2023).

In summary, we found that septins are important for exocyst targeting to the division site during late stages of cytokinesis through multivalent interactions between septins and the exocyst subunits. The proper exocyst localization at the rim of the division plane is critical for timely and successful cytokinesis. Our results will provide insights into future studies of the interactions and functions of septins and the exocyst complex in other cell types.

Materials and methods

Strains and molecular methods

Fission yeast strains used in this study are listed in Supplemental Table S1. Strains were constructed using PCR-based gene targeting and standard genetic methods (Moreno et al., 1991; Bähler et al., 1998). Tagged genes were expressed under endogenous promoters and integrated at their native chromosomal loci except where noted. The glucan synthase gene *bgs1* is integrated at the *leu1* loci under endogenous promoter, with the endogenous copy deleted (Cortes et al., 2002).

The functionalities of the tagged proteins (Spn1, Sec3, Exo70, Spn2, Sec5, Sec6, and Sec15) were tested by growing the strains at 25°C and 36°C on YE5S media or crossing to mutants. The growth and morphology of majority of the tagged strains were comparable to WT. However, Spn1 fused to red fluorescence tag (tdTomato and mCherry) localized abnormally to the plasma membrane on the cell sides at 25°C, indicating that these tagged proteins were not fully functional. tdTomato tagged Spn4 localized abnormally to the plasma membrane on the cell sides in addition to the division site. Although Spn4-mScarlet-I localized specifically to the division site, it is not fully functional with a small percentage of elongated and multiseptated cells at 25°C. These nonfunctional strains were not used.

Microscopy

Cells were normally grown at the exponential phase in YE5S liquid medium at 25°C for 40-48 h before microscopy or temperature shift. Confocal microscopy was performed as previously described (Wang et al., 2014; Davidson et al., 2015; Davidson et al., 2016; Zhu et al., 2018). Briefly, cells were collected from liquid culture by centrifuging at 3,000 rpm for 30 s at room temperature and washed with EMM5S twice to reduce autofluorescence. A final concentration of 50 nM *n*-propyl-gallate (*n*-PG) from a 10x stock (in EMM5S) was added in the second wash to protect cells from free radicals during imaging. Live cells were imaged on a thin layer of EMM5S with 20% gelatin and 50 nM *n*-PG at ~23°C. To image cells at 36°C, concentrated cells were grown in coverglass-bottom dish and covered with EMM5S agar (Davidson et al., 2016).

We imaged cells using two confocal microscopy systems with 100x/1.4 or 100x/1.45 numerical aperture (NA) Plan-Apo objective lenses (Nikon, Melville, NY). Most fluorescence images were taken using a PerkinElmer spinning disk confocal system (UltraVIEW Vox CSUX1 system; PerkinElmer, Waltham, MA) with 440-, 488-, 515-, and 561-nm solid-state lasers and back thinned electron-multiplying charge-coupled device (EMCCD) cameras (C9100-13 or C9100-23B; Hamamatsu Photonics, Bridgewater, NJ) on a Nikon Ti-E inverted microscope. For better spatial resolution, **Figure 1A** was imaged using another spinning disk confocal microscope (UltraVIEW ERS; PerkinElmer) with 568-nm solid-state laser and 488-nm argon ion lasers and a cooled charge-coupled device camera (ORCA-AG; Hamamatsu Photonics) on a Nikon Eclipse TE2000-U microscope. We used TIRF microscopy controlled by NIS Elements software to examine the dynamic localization of the exocyst subunit Exo70 and the septin Spn1 at the division site for some movies. A Nikon Eclipse Ti-E microscope equipped with a TIRF illuminator, Plan Apo 100x/1.45NA oil objective, and an Andor iXon Ultra 897 EMCCD was used.

Image analysis

We analyzed images using ImageJ (National Institutes of Health, Bethesda, MD) and Volocity (PerkinElmer). Fluorescence images are maximum-intensity projections from z-sections spaced at 0.5 µm except where noted. Images of 3D projections (end-on views) and deconvolution (**Figure 7C**, Eng1) were generated from images with z-sections spaced at 0.05 µm. For quantification of

fluorescence intensity at the division site, we summed the intensity from all z-sections using sum projection. A rectangular ROI1 was drawn to include majority of division site signal for intensity measurement. Then the intensity in a second ROI2 approximately twice the area of ROI1 (including ROI1) was measured and used to subtract cytoplasmic background as described previously (Coffman et al., 2011; Davidson et al., 2015; Davidson et al., 2016).

For comparing the colocalization at the rim of the division plane (**Figure 1B**), a line along the cell long-axis was drawn across the division plane at the same position for both Spn1 and Sec3 channels using maximum intensity projection images. Then the width of the line was adjusted to cover all signals at the division site, generating an ROI of 1.5 µm x 3.5 µm (x-y) (see **Figure 1B**). The mean intensity of all pixels in y-axis was measured along x-axis and plotted.

Line scans (**Figures 6D**, 7A, and 7C) across the division plane were made in the middle focal plane of the fluorescence images. A line along the cell short-axis was drawn across the division plane to cover the whole cell diameter. The width of the line was 3 pixels to reduce signal variations caused by measurements on a single focal plane. Mean intensity (average of 3 pixels) was measured across cell diameter. For Syb1 (**Figure 6D**), cells at the end of ring constriction (indicated by an Rlc1 dot at the center of the division plane) were measured; and line scans were aligned by referencing the peak intensity of Rlc1 signal. For Bgs1 (**Figure 7A**), cells with full septa were measured; and line scans were aligned by the peak intensity of Bgs1 signal. For Eng1 (**Figure 7C**), cells with full septa were measured; and line scans for WT cells were aligned by the middle of the two peaks; and the ones for *spn1*Δ cells were aligned by referencing the middle of septa in DIC images.

FRAP analysis

FRAP was performed using the photokinesis unit on the UltraVIEW Vox confocal system at either ~23°C or 36°C (Coffman et al., 2009; Laporte et al., 2011; Zhu et al., 2013). Half of the division site signals at the middle focal plane were photobleached to <50% of the original fluorescence intensity. Five pre-bleach images and 150 post-bleach images for *spn1*Δ cells, or 70 post-bleach images for *sec3-913* cells, were collected at every 0.33 s or 10 s, respectively. For image analysis, the background and photobleaching during image acquisition were corrected using empty space and unbleached cells within the same image. The pre-bleach intensity was normalized to 100%, and the first post-bleach intensity was normalized to 0% (Laporte et al., 2011; Zhu et al., 2018). Intensities of three consecutive post-bleach time points were rolling averaged to reduce noise (Vavylonis et al., 2008). Data were plotted and fitted using the exponential decay equation $y = m_1 + m_2 \exp(-m_3 x)$, where m_3 is the off-rate. The half-time for recovery was calculate by $t_{1/2} = \ln 2/m_3$.

Predictions of septin-exocyst interactions using AlphaFold analysis

The development of computer algorithms to predict three-dimensional protein structures from amino acid sequence involves two complementary ways that concentrate on either the physical interactions or the evolutionary history (Jumper et al., 2021). AlphaFold utilizes cutting-edge neural network topologies and training techniques to predict the 3D coordinates of a primary amino acid sequence (Jumper et al., 2021). We made the AlphaFold models of interactions between different septin and exocyst subunits using Google Colab Platform and AlphaFold2_advanced option that does not need templates at: *https://colab.research.google.com/github/sokrypton/ColabFold/blob/main/beta/AlphaFold2_advanced.ipynb#scrollTo=ITcPnLkLuDDE*. Sequences of each subunit were searched against genetic databases with msa_method = mmseqs2, pair_mode = unpaired. The default mode of sampling options was used; num_models = 5, ptm option, num_ensemble = 1, max_cycles = 3, num_samples = 1. Total 5 models were ranked according to their Predicted Local-Distance Difference Test (pLDDT) score between 0 to 100, from low to high confidence level. Septin and exocyst subunits were input in 1:1 ratio. For each of the 32 pairs of septin and exocyst subunits, the protein sequences were entered in both orders (for

example, Spn1:Sec3 and Sec3:Spn1). We found that the order of input sequence has effect on prediction results. So, we predicted all septin-exocyst combinations in both input sequence orders (septin first exocyst later and exocyst first septin later). We then selected the top septin-exocyst combinations that showed interactions in both input orders. The structure figures were drawn with PyMOL version 2.0 (Schrodinger, Inc.).

Co-IP and Western blotting

We carried out Co-IP and Western blotting as previously described (Laporte et al., 2011; Lee and Wu, 2012; Ye et al., 2012). Briefly, mEGFP, GFP, mYFP, or 13Myc tagged septin or exocyst subunits were expressed under native promotors in fission yeast. Cells were grown in YE5S liquid medium at 25°C for ~48 h before harvesting and lyophilization. Lyophilized cells (200 mg) were ground into a homogeneous fine powder using pestles and mortars. IP buffer (50 mM 4-(2-hydroxyethyl)-1-piperazineethanesulfonic acid [HEPES], pH 7.5, 150 mM NaCl, 1 mM EDTA, 0.1% NP-40, 50 mM NaF, 20 mM glycerophosphate, and 0.1 mM Na_3VO_4, 1 mM PMSF, and protease inhibitor [Roche] 1 tablet/30 ml buffer) was added according to the ratio of 10 µl: 1 mg lyophilized cell powder. 60 µl Dynabeads protein G beads (Invitrogen) were incubated with 5 µg polyclonal GFP antibody (Novus Bio) for 1 h at room temperature. After three washes with PBS and one wash with 1 ml IP buffer, the beads were incubated with cell lysate for 2 h at 4°C. After 5 washes at 4°C with 1 ml IP buffer each time, proteins were eluted by boiling with 80 µl sample buffer. The protein samples were separated with SDS-PAGE gel and detected with monoclonal anti-GFP antibody (1:1,000 dilution; 11814460001; Roche, Mannheim, Germany), monoclonal anti-Myc antibody (1:500 dilution, 9E10, Santa Cruz Biotechnology, Dallas, TX) and anti-tubulin TAT1 antibody (1:10,000 dilution)(Woods et al., 1989). Secondary antibody anti-mouse immunoglobulin G (1:5,000 dilution; A4416, Sigma-Aldrich) was detected using SuperSignal Maximum Sensitivity Substrate (Thermo Fisher Scientific) on iBright CL1500 imager (Thermo Fisher Scientific).

Electron microscopy

Electron microscopy was performed at the Boulder Electron Microscopy Services at the University of Colorado, Boulder (Boulder, CO) as previously described (Lee et al., 2014; Wang et al., 2016). Briefly, yeast cells were grown at 25°C for ~41 h and then shifted to 36°C for 4 h before harvesting using Millipore filters. Samples were prepared using high-pressure freezing with a Wohlwend Compact 02 Freezer in the presence of 2% osmium tetroxide and 0.1% uranyl acetate in acetone. Thin sections with a thickness of 70 nm were cut and embedded in Epon-Araldite epoxy resin, which were post stained with uranyl acetate and lead citrate. Imaging of EM samples was done using a Philips CM100 transmission electron microscope (FEI, Hillsboro, OR).

Yeast two hybrid assays

Yeast two hybrid assays were performed as described previously using X-gal overlay and β-D-galactosidase activity quantifications (Amberg et al., 2006; Paiano et al., 2019). DNA or cDNA (for genes with introns) sequences of Spn1, Spn1(aa 300-469), Spn2, Spn4, Sec15, Sec5, and Sec6 were cloned into pVP16 or pGBT9 vectors having VP16 transcription activation domain (AD) or GAL4 transcription factor DNA-binding domain (BD), respectively. Constructed plasmids were confirmed by restriction digestions and Sanger sequencing. Pairs of plasmids were then co-transformed into *S. cerevisiae* strain MAV203 (11281-011; Invitrogen) and plated on synthetic drop-out medium lacking leucine and tryptophan (SD-L-W) for selection. For X-gal overlay assay, grown colonies were re-streaked on YPD (yeast extract-peptone-dextrose) plates to grow overnight. We used 10-12 ml chloroform per plate to permeabilize cells for 10 min and then dried for additional 10 min. 0.5% agarose was prepared in 25 ml PBS (pH 7.5) and 500 µl X-gal (20 mg/ml stock in DMSO) was added after cooling. After mixing thoroughly, agarose containing X-gal was overlaid onto the colonies and incubated at 30°C. Plates were checked every 30 min for development of blue color.

Interactions were then quantified by β-D-galactosidase activity using the *o*-nitrophenyl– β-D-galactopyranoside (ONPG) assay (48712-M; Sigma Aldrich) according to the published methods (Amberg et al., 2006; Paiano et al., 2019). For interactions between Sec15 with Spn1, Spn2, and Spn4, the Amberg et al. method was used (Amberg et al., 2006). Briefly, cells were grown in SD-L-W liquid medium at 30°C overnight. 40 ml culture with OD_{595} >1 was collected and washed with 1 ml distilled water. Then cells were broken in 110 µl breaking buffer (100 mM Tris-Cl, pH 7.5, 1 mM DTT, and 20% glycerol) using glass beads on bead beater. 10 µl of the lysate was diluted with 90 µl distilled water and spun down to remove cell debris, and the supernatant was used to estimate protein concentration by Bradford assay. To the remaining 100 µl of lysate, 0.9 ml Z-buffer (100 mM sodium phosphate, pH 7.5, 10 mM KCl, and 2 mM $MgSO_4$) and 0.2 ml ONPG (8 mg/1 ml Z buffer) were added and incubated at 28°C until pale yellow color develops in at least one of the samples. All the reactions were stopped by adding 0.4 ml 1 M Na_2CO_3. Debris were removed by centrifuging at 15,700 g for 10 min and OD_{420} was measured using 1 ml of supernatant. Time elapsed from adding ONPG to adding stop solution was recorded and activity of β-galactosidase was calculated using the formula: β-galactosidase activity (nmol/min/mg) = OD_{420} × 1.7/ [0.0045 × protein (mg/ml) × extract volume (ml) × time (min)]

For the interaction between Spn1 and Sec6, the Painano et al. method was used (Paiano et al., 2019). Briefly, cultures were diluted to OD_{595} = 0.30 and incubated for 2 hrs at 30°C. For each sample, cells from 9 ml culture were collected and washed with 1 ml Z buffer and then resuspended in 0.1 ml Z buffer. Cells were broken by three freeze-thaw cycles in liquid nitrogen. 0.7 ml Z buffer with β-mercaptoethanol (27 µl β-mercaptoethanol in 9.973 ml Z buffer) and 160 µl ONPG was added to the cell lysates and incubated at 30°C until a yellow color develop in at least one of the samples. Reactions were stopped by adding 0.4 ml 1 M Na_2CO_3. Debris were removed by centrifuging at 15,700 g for 10 min and OD_{420} was measured using 1 ml of supernatant. Time elapsed from adding ONPG to adding stop solution was recorded and β-galactosidase activity were calculated using following formula: β-galactosidase Units = 1000 × OD_{420}/ [T × V × OD_{595}], where T is the elapsed time (minutes), V is the volume (ml) of culture used, and OD595 is the optical density of yeast culture.

Statistical analysis

Data in graphs are mean ± 1 SD except where noted. The *p*-values in statistical analyses were calculated using the two-tailed Student's *t* tests except **Figure 4**. The P values in **Figure 4** (E and F) was calculated using one way ANOVA with Tukey's post hoc test for quantification of yeast two hybrid analysis. Data is shown in Mean ± SD except where noted.

Supplemental material

Fig S1 shows localization, levels, and dynamics of septin and exocyst subunits. Fig S2 shows localization of Sec3 and Spn1 in *gef3*, *rho4*, and *gef3 rho4* mutants. Fig S3 presents Alphafold predicted models of septin and exocyst subunit interactions. Fig S4 shows that septin subunits interact with exocyst subunits in reciprocal Co-IP. Video 1 shows accumulation of Spn1-mEGFP to the division site with the exocyst Exo70-tdTomato. Video 2 and 3 represents the dynamic localization of Exo70-tdTomato at the division site. Video 4 shows the localization of Sec15-mEGFP as a ring in WT cells. Video 5 and 6 shows the mislocalization of Sec15-mEGFP from a ring to disc on division plane with deletion of *spn1* and *spn4* respectively during late-stage of cytokinesis.

Additional information

Funding

Pelotonia Graduate Fellowship to Yajun Liu, and the National Institute of General Medical Sciences of NIH grant GM118746 to Jian-Qiu Wu.

Author Contributions

Performed the experiments, methodology, validation, and formal data analysis: D. Singh, Y. Liu, Y.-H. Zhu, S. Zhang, S. Naegele. Visualization, figure and table preparations: D. Singh and Y. Liu. Writing and editing manuscript: Y. Liu, D. Singh, and J-Q Wu. Supervision, conceptualization, investigation, review: J.Q. Wu. Funding acquisition: Y. Liu and J-Q Wu.

Competing Interest

The authors declare no competing interest.

Abbreviations used in this paper

- Co-IP: Co-immunoprecipitation
- EMCCD: Electron-multiplying charge-coupled device
- FPS: Frame per second
- FRAP: Fluorescence recovery after photobleaching
- NA: Numerical aperture
- PB: Phloxin B
- pLDDT: Predicted Local-Distance Difference Test
- ROI: Region of interest
- SPB: Spindle pole body
- TIRF: Total internal reflection fluorescence
- TRAPP-II: Transport particle protein-II
- WT: Wild type

Acknowledgements

We thank Pilar Pérez for strains; Eileen O'Toole and Garry Morgan at University of Colorado, Boulder for help with electron microscopy; Anita Hopper, Steve Osmani, Dmitri Kudryashov, Elena Kudryashova, Damien Wilburn, and Emily Vais for equipment and technical support; and members of the Wu laboratory for helpful discussion and suggestions.

Supplementary figures

Strain	Genotype	Figure/Reference
JW8692	*sec3-tdTomato-hphMX6 spn1-mEGFP-kanMX6 sad1-mRFP1-kanMX6 ade6-M210 leu1-32 ura4-D18*	Figure 1, A-D
JW1113	*h⁻ spn1-mEGFP-kanMX6 sad1-mRFP1-kanMX6 ade6-M210 leu1-32 ura4-D18*	Figure 1E
JW1100	*spn1-mEGFP-kanMX6 ade6-M210 leu1-32 ura4-D18*	Figures 1, G and H; 4C; S2B; S4A
JW8928	*spn1-mEGFP-kanMX6 sec3-913-hphMX6 ade6 leu1-32 ura4-D18*	Figures 1, E, G and H; S1, A, C and E
JW8848	*sec8-1 spn1-mEGFP-kanMX6 sad1-mRFP1-kanMX6 rng8-tdTomato-kanMX6 ade6-M210 leu1-32 ura4-D18*	Figure 1F
JW6149	*h⁺ sec3-GFP-kanMX6 ade6-M216 leu1-32 ura4-D18*	Figures 2, A-C; S1I; S2A
JW7322	*spn1-Δ2::kanMX6 sec3-GFP-kanMX6 ade6-M216 leu1-32 ura4-D18*	Figures 2, A-C; S1I
JW7061	*h⁻ sec8-GFP-ura4⁺ rlc1-tdTomato-natMX6 ade6? leu1-32 ura4-D18*	Figures 2, D and E; S1, G and H
JW8295	*sec8-GFP-ura4⁺ rlc1-tdTomato-natMX6 spn1-Δ2::kanMX6 leu1-32 ura4-D18*	Figures 2, D and E; S1, G and H
JW9737	*h⁺ spn2-mEGFP-kanMX6 ade6-M210 ura4-D18 leu1-32*	Figure 4A
JW9731	*h⁻ sec15-13Myc-kanMX6 ade6-210 ura4-D18 leu1-32*	Figures 4, A and C; S4E
JW9757	*spn2-mEGFP-kanMX6 sec15-13Myc-kanMX6 ade6-M210 ura4-D18 leu1-32*	Figure 4A
JW9756	*h⁺ spn2-13Myc-kanMX6 ade6-M210 leu1-32 ura4-D18*	Figure 4B
JW9726	*h⁻ sec15-mEGFP-kanMX6 ade6-210 ura4-D18 leu1-32*	Figure 4, B and D; Video 4
JW9771	*spn2-13Myc-kanMX6 sec15-mEGFP-kanMX6 ade6-210 ura4-D18 leu1-32*	Figure 4B
JW9744	*h⁺ spn1-mEGFP-kanMX6 sec15-13Myc-kanMX6 ade6-M210 leu1-32 ura4-D18*	Figure 4C
JW9733	*h⁻ spn1-13Myc-hphMX6 sec15-mEGFP-kanMX6 ade6-M210 ura4-D18 leu1-32*	Figure 4D
JW8596	*h⁺ spn1-13Myc-hphMX6 ade6-M210 leu1-32 ura4-D18*	Figures 4D; S4B
JW9789	*h⁺ spn2-Δ1::hphMX6 sec15-mEGFP-kanMX6 ade6-210 ura4-D18 leu1-32*	Figure 5, A and B
JW9759	*h⁺ sec15-mEGFP-kanMX6 ade6-210 ura4-D18 leu1-32*	Figures 5, A and B; S4F
JW9853	*sec15-mEGFP-kanMX6 spn4-Δ2::hphMX6 ade6-M210 ura4-D18 leu1-32*	Figure 5, A and B; Video 5
JW9852	*sec15-mEGFP-kanMX6 spn1-Δ2::kanMX6 ade6-M210? ura4-D18 leu1-32*	Figure 5, A and B; Video 6

Supplemental Table 1.

***S. pombe* strains used in this study.**

JW9804	*spn2-Δ1::hphMX6 sec5-mEGFP-kanMX6 ade6-210 ura4-D18 leu1-32*	Figure 5, C and D
JW9791	*h^+ sec5-mEGFP-kanMX6 ade6-M210 ura4-D18 leu1-32*	Figure 5, C and D
JW81	*h^- ade6-210 ura4-D18 leu1-32*	Figures 6, A and B; 7B
JW289	*h^+ spn1-Δ2::kanMX6 leu1-32 ura4-D18*	Figures 6, A and B; 7B; Table 1
JW3915	*h^+ sec8-1 ura4-D18 leu1-32*	Figures 6, A and B; 7B
JW7130	*h^- kanMX6-Pypt3-mEGFP-ypt3 ade6-210 leu1-32 ura4-D18*	Figure 6C
JW7354	*spn1-Δ2::kanMX6 kanMX6-Pypt3-mEGFP-ypt3 leu1-32 ura4-D18*	Figure 6C
JW6548	*h^+ GFP-syb1-kanMX6 rlc1-tdTomato-natMX6 ade6 leu1-32 ura4-D18*	Figure 6D
JW7385	*spn1-Δ2::kanMX6 GFP-syb1-kanMX6 rlc1-tdTomato-natMX6 leu1-32 ura4-D18*	Figure 6D
JW5249	*GFP-bgs1-leu1$^+$ bgs1Δ::ura4$^+$ rlc1-tdTomato-natMX6 ade6-M210 leu1-32 ura4-D18*	Figure 7A
JW7264	*GFP-bgs1-leu1$^+$ bgs1Δ::ura4$^+$ rlc1-tdTomato-natMX6 spn1-Δ2::kanMX6 ade6 ura4-D18*	Figure 7A
JW6192	*h^- eng1-GFP-kanR leu1-32 ura4-D18*	Figure 7C (Santos et al., 2005)
JW9057	*eng1-GFP-kan^R spn1-Δ2::kanMX6 leu1-32 ura4-D18*	Figure 7C
JW1113	*h^- spn1-mEGFP-kanMX6 sad1-mRFP1-kanMX6 ade6-M210 leu1-32 ura4-D18*	Figure S1, A, C-E;
JW8829	*exo70Δ::kanMX4 spn1-mEGFP-kanMX6 sad1-mRFP1-kanMX6 ade6 leu1-32 ura4-D18*	Figure S1, A-D
JW8830	*sec8-1 spn1-mEGFP-kanMX6 sad1-mRFP1-kanMX6 ade6-M210 leu1-32 ura4-D18*	Figure S1, A-D
JW8929	*h^- exo70-mEGFP-kanMX6 ade6-M210 ura4-D18 leu1-32*	Figure S1, F and H
JW8960	*exo70-mEGFP-kanMX6 spn1-Δ2::kanMX6 ade6-M210 leu1-32 ura4-D18*	Figure S1, F and H
JW8938	*rho4Δ::kanMX6 sec3-GFP-kanMX6 leu1-32 ura4-D18*	Figure S2A
JW8955	*gef3Δ::hphMX6 sec3-GFP-kanMX6 ade6-M210 leu1-32 ura4-D18*	Figure S2A
JW8959	*gef3Δ:: hphMX6 rho4Δ::kanMX4 sec3-GFP-kanMX6 ade6? leu1-32? ura4-D18*	Figure S2A
JW9058	*gef3Δ:: hphMX6 rho4Δ::kanMX4 spn1-mEGFP-kanMX6 ade6 leu1-32 ura4-D18*	Figure S2B
JW9765	*h^- sec6-13Myc-kanMX6 ade6-210 ura4-D18 leu1-32*	Figure S4A
JW9774	*spn1-mEGFP-kanMX6 sec6-13Myc-kanMX6 ade6-M210 leu1-32 ura4-D18*	Figure S4A
JW9766	*h^- sec6-mEGFP-kanMX6 ade6-210 ura4-D18 leu1-32*	Figure S4B

Supplemental Table 1. (continued)

JW9832	*spn1-13Myc-hphMX6 sec6-mEGFP-kanMX6 ade6-210 ura4-D18 leu1-32*	Figure S4B
JW8778	*h⁻ spn2-mEGFP-kanMX6 ade6-M210 leu1-32 ura4-D18*	Figure S4C
JW9755	*h⁺ sec5-13Myc-kanMX6 ade6-M210 leu1-32 ura4-D18*	Figure S4C
JW9772	*sec5-13Myc-kanMX6 spn2-mEGFP-kanMX6 ade6-210 ura4-D18 leu1-32*	Figure S4C
JW9756	*h⁺ spn2-13Myc-kanMX6 ade6-M210 leu1-32 ura4-D18*	Figure S4D
JW9738	*h⁻ sec5-mEGFP-kanMX6 ade6-M210 ura4-D18 leu1-32*	Figure S4D
JW9775	*spn2-13Myc-kanMX6 sec5-mEGFP-kanMX6 ade6-M210 leu1-32 ura4-D18*	Figure S4D
JW1171	*h⁺ spn4-mYFP-kanMX6 ade6-M210 leu1-32 ura4-D18*	Figure S4, E and G
JW9829	*sec15-13Myc-kanMX6 spn4-mYFP-kanMX6 ade6-M210 ura4-D18 leu1-32*	Figure S4E
JW9854	*spn4-13Myc-kanMX6 sec15-mEGFP-kanMX6 ade6-210 ura4-D18 leu1-32*	Figure S4F
JW9768	*h⁻ spn4-13Myc-kanMX6 ade6-210 ura4-D18 leu1-32*	Figure S4, F and H
JW9139	*h⁻ sec3-13Myc-natMX6 ade6-210 leu1-32 ura4-D18*	Figure S4G
JW9711	*spn4-mYFP-kanMX6 sec3-13Myc-natMX6 ade6-M210 leu1-32 ura4-D18*	Figure S4G
JW7300	*h⁺ sec3-GFP-kanMX6 ade6-M210 leu1-32 ura4-D18*	Figure S4H
JW9788	*spn4-13Myc-kanMX6 sec3-GFP-kanMX6 ade6-210 leu1-32 ura4-D18*	Figure S4H
JW7035	*h⁻ trs120-M1-his5⁺-kanMX6 his5Δ ade6-M210 leu1-32 ura4*	Tables 1 and 2
JW8821	*trs120-M1-his5⁺-kanMX6 spn1-Δ2::kanMX6 leu1-32 ura4*	Tables 1 and 2
JW7036	*h⁻ trs120-ts1-his5⁺-kanMX6 his5Δ ade6-M210 leu1-32 ura4*	Tables 1 and 2
JW8822	*trs120-ts1-his5⁺-kanMX6 spn1-Δ2::kanMX6 leu1-32 ura4*	Tables 1 and 2
JW290	*h⁻ spn1-Δ2::kanMX6 his3-27 ura4-D18*	Tables 1 and 2
JW3915	*h⁺ sec8-1 ura4-D18 leu1-32*	Tables 1 and 2
JW8796	*spn1-Δ2::kanMX6 sec8-1 ura4-D18*	Tables 1 and 2
JW2716	*h⁺ exo70Δ::kanMX4 ade6 leu1-32 ura4-D18*	Tables 1 and 2
JW8797	*spn1-Δ2::kanMX6 exo70Δ::kanMX4 his3-27 ade6 ura4-D18*	Tables 1 and 2
JW6148	*h⁻ sec3-916-hphMX6 ade6-M216 leu1-32 ura4-D18*	Tables 1 and 2
JW8787	*spn1-Δ2::kanMX6 sec3-916-hphMX6 ade6-M216 leu1-32 ura4-D18*	Tables 1 and 2
JW6147	*h⁻ sec3-913-hphMX6 ade6-M216 leu1-32 ura4-D18*	Tables 1 and 2
JW8783	*spn1-Δ2::kanMX6 sec3-913-hphMX6 ade6-M216 leu1-32 ura4-D18*	Tables 1 and 2

Supplemental Table 1. (continued)

JW8588	*spn2-Δ1::ura4*$^{+}$ *ade6 leu1-32 ura4-D18*	Tables 1 and 2
JW8782	*spn2-Δ1::ura4*$^{+}$ *sec3-913-hphMX6 ade6 leu1-32 ura4-D18*	Tables 1 and 2
JW8789	*spn2-Δ1::ura4*$^{+}$ *sec3-916-hphMX6 ade6 leu1-32 ura4-D18*	Tables 1 and 2
JW6148	*h*$^{+}$ *spn3-Δ2::kanMX6 ade6-M210 leu1-32 ura4-D18*	Tables 1 and 2
JW8790	*spn3-Δ2::kanMX6 sec3-913-hphMX6 ade6-M21X leu1-32 ura4-D18*	Tables 1 and 2
JW8785	*spn3-Δ2::kanMX6 sec3-916-hphMX6 ade6-M21X leu1-32 ura4-D18*	Tables 1 and 2
JW293	*h*$^{-}$ *spn4-Δ2::kanMX6 ura4-D18*	Tables 1 and 2
JW295	*h*$^{+}$ *spn4-Δ2::kanMX6 leu1-32 ura4-D18*	Tables 1 and 2
JW8784	*spn4-Δ2::kanMX6 sec3-913-hphMX6 ade6-M216 leu1-32 ura4-D18*	Tables 1 and 2
JW8788	*spn4-Δ2::kanMX6 sec3-916-hphMX6 leu1-32 ura4-D18*	Tables 1 and 2
JW8799	*spn4-Δ2::kanMX6 sec8-1 leu1-32 ura4-D18*	Tables 1 and 2
JW9170	*spn1-mEGFP-kanMX6 exo70-tdTomato-natMX6 ade6-M210 leu1-32 ura4-D18*	Video 1-3

Supplemental Table 1. (continued)

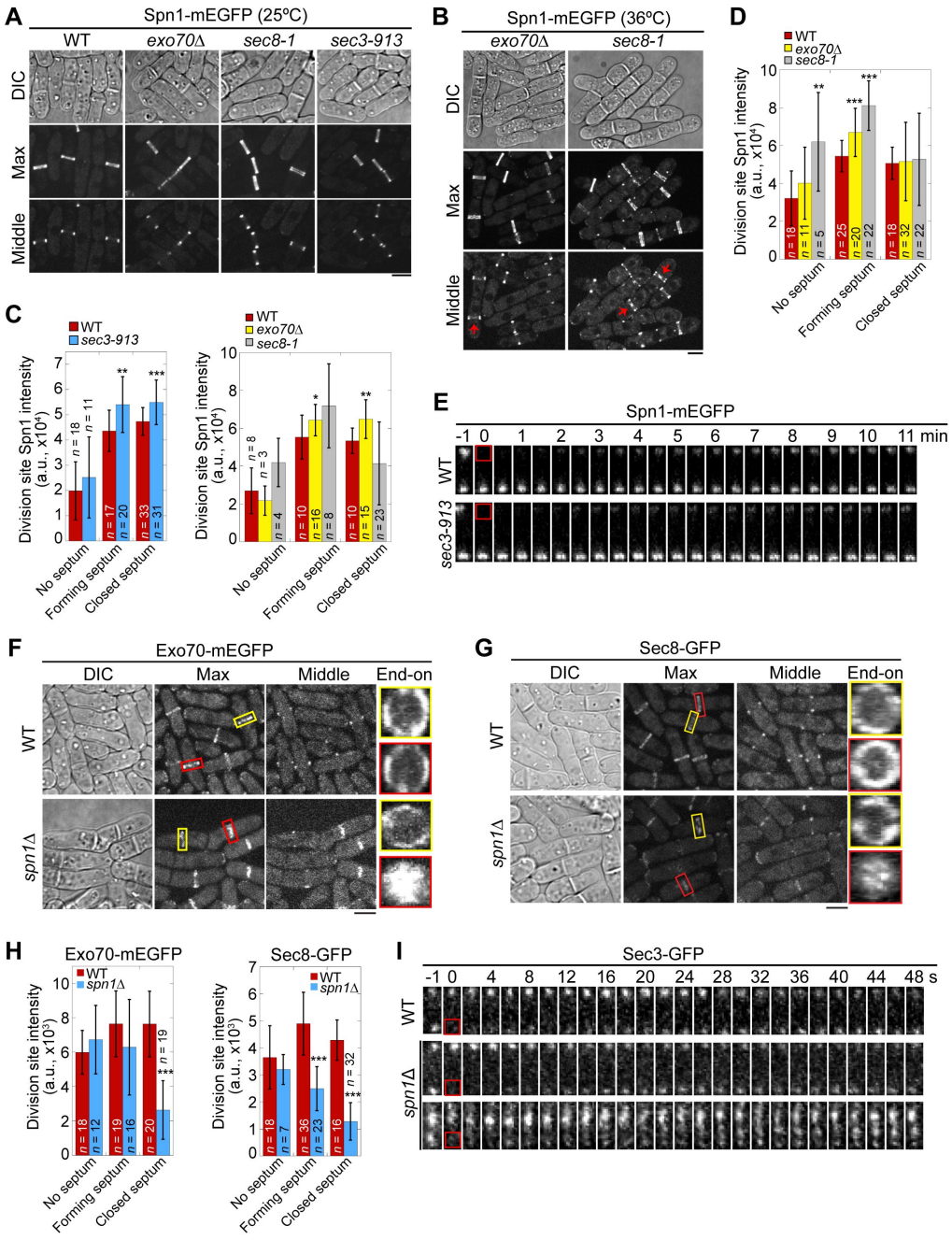

Figure S1.

Localization and division site levels of septin and exocyst subunits in mutants; and FRAP analyses of Spn1 and Sec3. (A and B)

Localization of Spn1 in WT and exocyst mutants at 25°C (A) and 4 h at 36°C (B). Arrows indicate cells with mislocalized Spn1 at the center of the division plane. **(C and D)** Quantifications of Spn1 intensities at the division site in WT and exocyst mutants at 25°C (C) and 4 h at 36°C (D). No septum: cells with Spn1 signal at the division site but no septum is visible under DIC; forming septum: septum with a visible gap in the middle; closed septum: no visible gap in the septum. *, P < 0.05; **, P < 0.01; ***, P < 0.001. **(E)** FRAP analyses of Spn1 at the division site in WT and *sec3-913* cells grown at 36°C for 4 h. Time-lapse images show recovery of Spn1 signals over time. Red box marks the region photobleached at time 0. **(F and G)** Localization of Exo70 (F) and Sec8 (G) in WT and *spn1*Δ cells. Yellow boxes, cells without a septum; Red boxes, cells with a closed septum. **(H)** Quantifications of Exo70 (left) and Sec8 (right) intensities at the division site in WT and *spn1*Δ cells. ***, P < 0.001. **(I)** FRAP analyses of Sec3 at the division site in WT and *spn1*Δ cells. Red box marks the region photobleached at time 0. Bars, 5 μm.

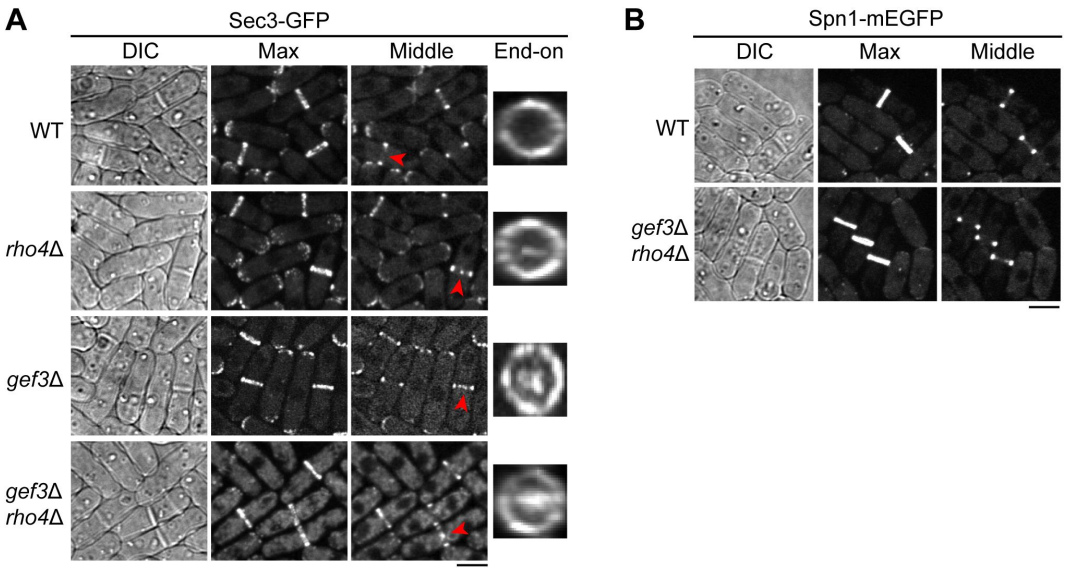

Figure S2.

Sec3 and Spn1 localization in *gef3*, *rho4,* or *gef3 rho4* mutants. (A)

Sec3 localization in WT, *rho4*Δ, *gef3*Δ, and *gef3*Δ *rho4*Δ cells. Arrowheads mark examples of the cells with mislocalized Sec3 at the center of the division plane in mutant but not WT cells. End-on views of the division plane of cells with a closed septum are shown on the last column. **(B)** Spn1 localization in WT and *gef3*Δ *rho4*Δ cells. Bars, 5 μm.

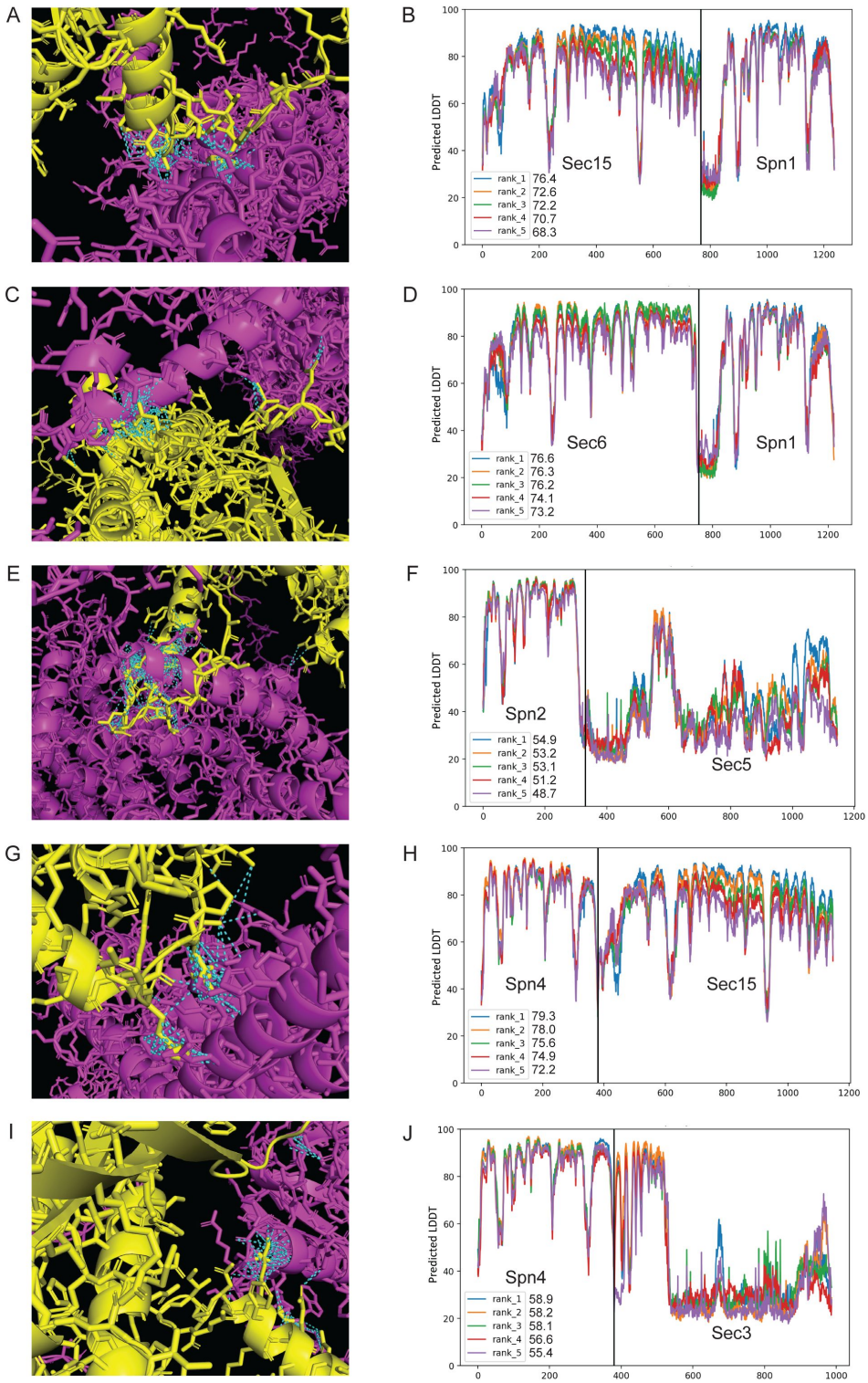

Figure S3.

The 3D structural models of septin-exocyst interactions generated by AlphaFold. (A, C, E, G, I)

Rank 1 model of AlphaFold2_advanced predicted interaction between Sec15 and Spn1 (A), Sec6 and Spn1 (C), Spn2 and Sec5 (E), Spn4 and Sec15 (G), and Spn4 and Sec3 (I). Septin subunits are colored in yellow and exocyst in magenta, contacts between interface residues with distance < 4 Å are colored in cyan. **(B, D, F, H, J)** pLDDT scores of five predicted models for Sec15 and Spn1 (B), Sec6 and Spn1 (D), Spn2 and Sec5 (F), Spn4 and Sec15 (H), and Spn4 and Sec3 (J).

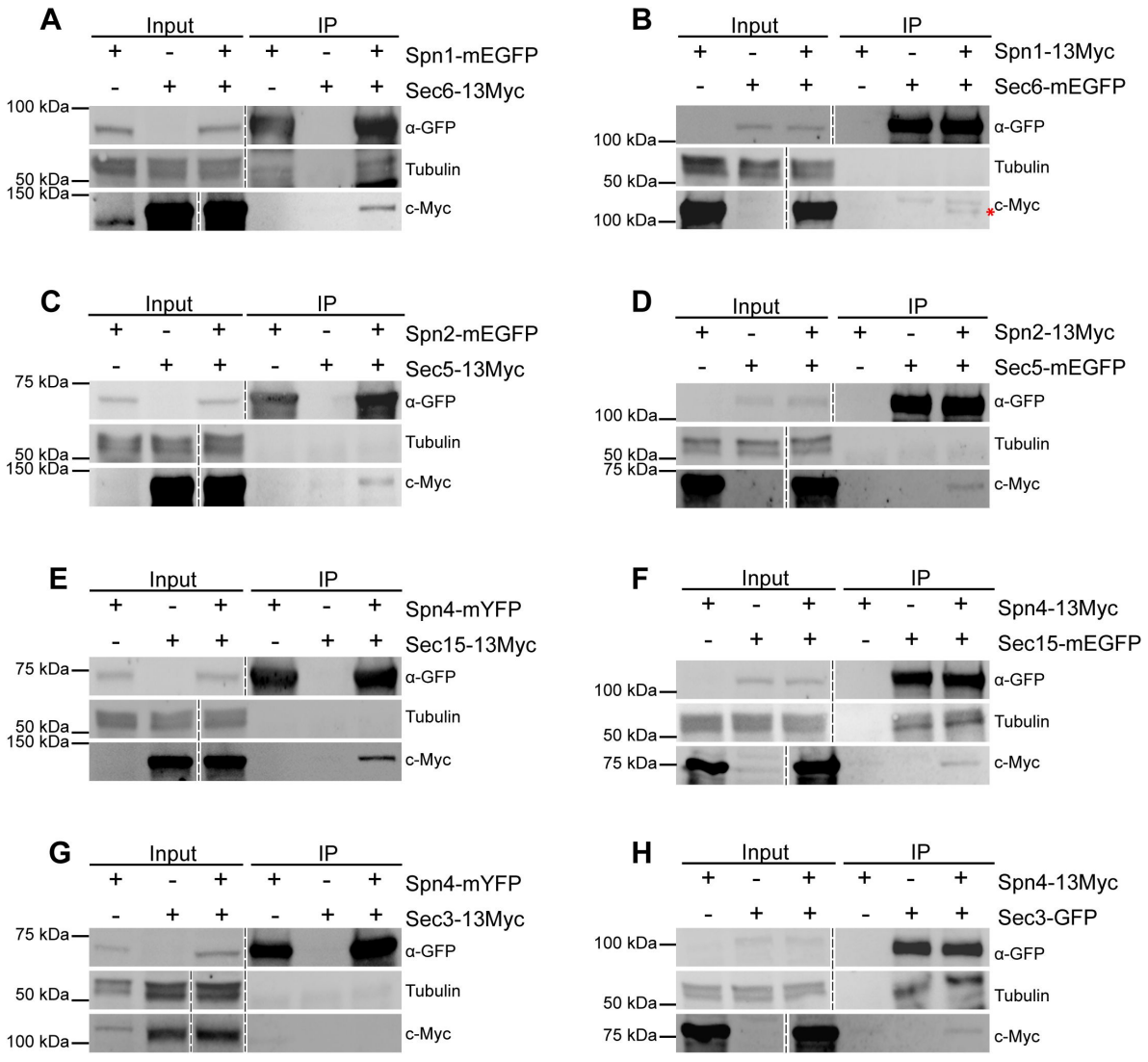

Figure S4.

Septins and exocyst interact physically.

Reciprocal co-immunoprecipitation between Spn1 with Sec6 **(A, B)**; Spn2 with Sec5 **(C, D)**; Spn4 with Sec15 **(E, F)**; and Spn4 with Sec3 **(G, H)**. Septin or exocyst subunits tagged with mEGFP, GFP, mYFP, or 13Myc were immunoprecipitated, separated on SDS-PAGE, and incubated with appropriate antibodies. Tagged proteins were detected on iBright Imager. Tubulin was used as a loading control. Asterisk (*) in B marks Spn1-13Myc. The dashed vertical lines mark the positions of protein ladders which was excised out.

References

1. Ageta-Ishihara N, Kinoshita M. (2021) **Developmental and postdevelopmental roles of septins in the brain** *Neurosci Res* **170**:6–12

2. Ahmed SM, Nishida-Fukuda H, Li Y, McDonald WH, Gradinaru CC, Macara IG (2018) **Exocyst dynamics during vesicle tethering and fusion** *Nat Commun* **9**

3. Amberg DC, Burke DJ, Strathern JN (2006) **Assay of β-galactosidase in yeast: assay of crude extracts** *Cold Spring Harb Protoc* **2006**

4. An H, Morrell JL, Jennings JL, Link AJ, Gould KL (2004) **Requirements of fission yeast septins for complex formation, localization, and function** *Mol Biol Cell* **15**:5551–5564

5. Bähler J, Wu J-Q, Longtine MS, Shah NG, McKenzie A III, Steever AB, Wach A, Philippsen P, Pringle JR (1998) **Heterologous modules for efficient and versatile PCR-based gene targeting in Schizosaccharomyces pombe** *Yeast* **14**:943–951

6. Baladrón V, Ufano S, Dueñas E, Martín-Cuadrado AB, del Rey F, Vázquez de Aldana CR (2002) **Eng1p, an endo-1,3-beta-glucanase localized at the daughter side of the septum, is involved in cell separation in Saccharomyces cerevisiae** *Eukaryot Cell* **1**:774–786

7. Beites CL, Xie H, Bowser R, Trimble WS (1999) **The septin CDCrel-1 binds syntaxin and inhibits exocytosis** *Nat Neurosci* **2**:434–439

8. Bendezu FO, Martin SG (2011) **Actin cables and the exocyst form two independent morphogenesis pathways in the fission yeast** *Mol Biol Cell* **22**:44–53

9. Bendezu FO, Vincenzetti V, Martin SG (2012) **Fission yeast Sec3 and Exo70 are transported on actin cables and localize the exocyst complex to cell poles** *PLoS One* **7**

10. Berlin A, Paoletti A, Chang F (2003) **Mid2p stabilizes septin rings during cytokinesis in fission yeast** *J Cell Biol* **160**:1083–1092

11. Bertin A, McMurray MA, Grob P, Park SS, Garcia G, Patanwala I, Ng HL, Alber T, Thorner J, Nogales E (2008) **Saccharomyces cerevisiae septins: supramolecular organization of heterooligomers and the mechanism of filament assembly** *Proc Natl Acad Sci U S A* **105**:8274–8279

12. Bertin A, McMurray MA, Thai L, Garcia G, Votin V, Grob P, Allyn T, Thorner J, Nogales E (2010) **Phosphatidylinositol-4,5-bisphosphate promotes budding yeast septin filament assembly and organization** *J Mol Biol* **404**:711–731

13. Bi E, Maddox P, Lew DJ, Salmon ED, McMillan JN, Yeh E, Pringle JR (1998) **Involvement of an actomyosin contractile ring in Saccharomyces cerevisiae cytokinesis** *J. Cell Biol* **142**:1301–1312

14. Boyd C, Hughes T, Pypaert M, Novick P (2004) **Vesicles carry most exocyst subunits to exocytic sites marked by the remaining two subunits, Sec3p and Exo70p** *J Cell Biol* **167**:889–901

15. Bridges AA, Gladfelter AS (2016) **In vitro reconstitution of septin assemblies on supported lipid bilayers** *Methods Cell Biol* **136**:57–71

16. Bridges AA, Zhang H, Mehta SB, Occhipinti P, Tani T, Gladfelter AS (2014) **Septin assemblies form by diffusion-driven annealing on membranes** *Proc Natl Acad Sci U S A* **111**:2146–2151

17. Cannon KS, Woods BL, Crutchley JM, Gladfelter AS (2019) **An amphipathic helix enables septins to sense micrometer-scale membrane curvature** *J Cell Biol* **218**:1128–1137

18. Cannon KS, Woods BL, Gladfelter AS (2017) **The Unsolved Problem of How Cells Sense Micron-Scale Curvature** *Trends Biochem Sci* **42**:961–976

19. Cao L, Ding X, Yu W, Yang X, Shen S, Yu L (2007) **Phylogenetic and evolutionary analysis of the septin protein family in metazoan** *FEBS Lett* **581**:5526–5532

20. Carim SC, Hickson GRX (2023) **The Rho1 GTPase controls anillo-septin assembly to facilitate contractile ring closure during cytokinesis** *iScience* **26**

21. Caudron F, Barral Y (2009) **Septins and the lateral compartmentalization of eukaryotic membranes** *Dev Cell* **16**:493–506

22. Coffman VC, Nile AH, Lee IJ, Liu H, Wu J-Q (2009) **Roles of formin nodes and myosin motor activity in Mid1p-dependent contractile-ring assembly during fission yeast cytokinesis** *Mol Biol Cell* **20**:5195–5210

23. Coffman VC, Wu P, Parthun MR, Wu J-Q (2011) **CENP-A exceeds microtubule attachment sites in centromere clusters of both budding and fission yeast** *J Cell Biol* **195**:563–572

24. Cortes JC, Ishiguro J, Duran A, Ribas JC (2002) **Localization of the (1,3)beta-D-glucan synthase catalytic subunit homologue Bgs1p/Cps1p from fission yeast suggests that it is involved in septation, polarized growth, mating, spore wall formation and spore germination** *J Cell Sci* **115**:4081–4096

25. Dagdas YF, Yoshino K, Dagdas G, Ryder LS, Bielska E, Steinberg G, Talbot NJ (2012) **Septin-mediated plant cell invasion by the rice blast fungus, Magnaporthe oryzae** *Science* **336**:1590–1595

26. Davidson R, Laporte D, Wu JQ (2015) **Regulation of Rho-GEF Rgf3 by the arrestin Art1 in fission yeast cytokinesis** *Mol Biol Cell* **26**:453–466

27. Davidson R, Liu Y, Gerien KS, Wu JQ (2016) **Real-Time Visualization and Quantification of Contractile Ring Proteins in Single Living Cells** *Methods Mol Biol* **1369**:9–23

28. DeMarini DJ, Adams AE, Fares H, De Virgilio C, Valle G, Chuang JS, Pringle JR (1997) **A septin-based hierarchy of proteins required for localized deposition of chitin in the Saccharomyces cerevisiae cell wall** *J Cell Biol* **139**:75–93

29. Dobbelaere J, Barral Y (2004) **Spatial coordination of cytokinetic events by compartmentalization of the cell cortex** *Science* **305**:393–396

30. Dobbelaere J, Gentry MS, Hallberg RL, Barral Y (2003) **Phosphorylation-dependent regulation of septin dynamics during the cell cycle** *Dev Cell* **4**:345–357

31. Dolat L, Hu Q, Spiliotis ET (2014) **Septin functions in organ system physiology and pathology** *Biol Chem* **395**:123–141

32. Du Y, Mpina MH, Birch PR, Bouwmeester K, Govers F (2015) **Phytophthora infestans RXLR Effector AVR1 Interacts with Exocyst Component Sec5 to Manipulate Plant Immunity** *Plant Physiol* **169**:1975–1990

33. Fang X, Luo J, Nishihama R, Wloka C, Dravis C, Travaglia M, Iwase M, Vallen EA, Bi E (2010) **Biphasic targeting and cleavage furrow ingression directed by the tail of a myosin II** *J Cell Biol* **191**:1333–1350

34. Feng S, Knödler A, Ren J, Zhang J, Zhang X, Hong Y, Huang S, Peränen J, Guo W (2012) **A Rab8 guanine nucleotide exchange factor-effector interaction network regulates primary ciliogenesis** *J Biol Chem* **287**:15602–15609

35. Finger FP, Hughes TE, Novick P (1998) **Sec3p is a spatial landmark for polarized secretion in budding yeast** *Cell* **92**:559–571

36. Finnigan GC, Booth EA, Duvalyan A, Liao EN, Thorner J (2015) **The Carboxy-Terminal Tails of Septins Cdc11 and Shs1 Recruit Myosin-II Binding Factor Bni5 to the Bud Neck in Saccharomyces cerevisiae** *Genetics* **200**:843–862

37. Ford SK, Pringle JR (1991) **Cellular morphogenesis in the Saccharomyces cerevisiae cell cycle: localization of the CDC11 gene product and the timing of events at the budding site** *Dev Genet* **12**:281–292

38. Frazier JA, Wong ML, Longtine MS, Pringle JR, Mann M, Mitchison TJ, Field C (1998) **Polymerization of purified yeast septins: evidence that organized filament arrays may not be required for septin function** *J Cell Biol* **143**:737–749

39. Fukai S, Matern HT, Jagath JR, Scheller RH, Brunger AT (2003) **Structural basis of the interaction between RalA and Sec5, a subunit of the sec6/8 complex** *EMBO J* **22**:3267–3278

40. Ganesan SJ, Feyder MJ, Chemmama IE, Fang F, Rout MP, Chait BT, Shi Y, Munson M, Sali A (2020) **Integrative structure and function of the yeast exocyst complex** *Protein Sci* **29**:1486–1501

41. Garcia G, Bertin A, Li Z, Song Y, McMurray MA, Thorner J, Nogales E (2011) **Subunit-dependent modulation of septin assembly: budding yeast septin Shs1 promotes ring and gauze formation** *J Cell Biol* **195**:993–1004

42. Gladfelter AS, Pringle JR, Lew DJ (2001) **The septin cortex at the yeast mother-bud neck** *Curr Opin Microbiol* **4**:681–689

43. Guo PP, Yong JY, Wang YM, Li CR (2016) **Sec15 links bud site selection to polarised cell growth and exocytosis in Candida albicans** *Sci Rep* **6**

44. Guo W, Roth D, Walch-Solimena C, Novick P (1999) **The exocyst is an effector for Sec4p, targeting secretory vesicles to sites of exocytosis** *EMBO J* **18**:1071–1080

45. Guo W, Tamanoi F, Novick P (2001) **Spatial regulation of the exocyst complex by Rho1 GTPase** *Nat Cell Biol* **3**:353–360

46. Gupta YK, Dagdas YF, Martinez-Rocha AL, Kershaw MJ, Littlejohn GR, Ryder LS, Sklenar J, Menke F, Talbot NJ (2015) **Septin-Dependent Assembly of the Exocyst Is Essential for Plant Infection by Magnaporthe oryzae** *Plant Cell* **27**:3277–3289

47. Haarer BK, Pringle JR (1987) **Immunofluorescence localization of the Saccharomyces cerevisiae CDC12 gene product to the vicinity of the 10-nm filaments in the mother-bud neck** *Mol Cell Biol* **7**:3678–3687

48. Halim DO, Munson M, Gao FB (2023) **The exocyst complex in neurological disorders** *Hum Genet* **142**:1263–1270

49. Hartwell LH (1971) **Genetic control of the cell division cycle in yeast** *IV. Genes controlling bud emergence and cytokinesis. Exp Cell Res* **69**:265–276

50. He B, Xi F, Zhang X, Zhang J, Guo W (2007) **Exo70 interacts with phospholipids and mediates the targeting of the exocyst to the plasma membrane** *EMBO J* **26**:4053–4065

51. Heider MR *et al.* (2016) **Subunit connectivity, assembly determinants and architecture of the yeast exocyst complex** *Nat Struct Mol Biol* **23**:59–66

52. Heider MR, Munson M (2012) **Exorcising the exocyst complex** *Traffic* **13**:898–907

53. Hernández-Rodríguez Y, Momany M (2012) **Posttranslational modifications and assembly of septin heteropolymers and higher-order structures** *Curr Opin Microbiol* **15**:660–668

54. Hsu SC, Hazuka CD, Roth R, Foletti DL, Heuser J, Scheller RH (1998) **Subunit composition, protein interactions, and structures of the mammalian brain sec6/8 complex and septin filaments** *Neuron* **20**:1111–1122

55. Hsu SC, TerBush D, Abraham M, Guo W (2004) **The exocyst complex in polarized exocytosis** *Int Rev Cytol* **233**:243–265

56. Hu Q, Nelson WJ (2011) **Ciliary diffusion barrier: the gatekeeper for the primary cilium compartment** *Cytoskeleton (Hoboken* **68**:313–324

57. Jin Y, Sultana A, Gandhi P, Franklin E, Hamamoto S, Khan AR, Munson M, Schekman R, Weisman LS (2011) **Myosin V transports secretory vesicles via a Rab GTPase cascade and interaction with the exocyst complex** *Dev Cell* **21**:1156–1170

58. Jourdain I, Dooley HC, Toda T (2012) **Fission yeast sec3 bridges the exocyst complex to the actin cytoskeleton** *Traffic* **13**:1481–1495

59. Jumper J *et al.* (2021) **Highly accurate protein structure prediction with AlphaFold** *Nature* **596**:583–589

60. Kartmann B, Roth D (2001) **Novel roles for mammalian septins: from vesicle trafficking to oncogenesis** *J Cell Sci* **114**:839–844

61. Kim DU *et al.* (2010) **Analysis of a genome-wide set of gene deletions in the fission yeast Schizosaccharomyces pombe** *Nat Biotechnol* **28**:617–623

62. Kim HB, Haarer BK, Pringle JR (1991) **Cellular morphogenesis in the Saccharomyces cerevisiae cell cycle: localization of the CDC3 gene product and the timing of events at the budding site** *J Cell Biol* **112**:535–544

63. Kinoshita M (2003) **Assembly of mammalian septins** *J Biochem (Tokyo* **134**:491–496

64. Kinoshita M, Kumar S, Mizoguchi A, Ide C, Kinoshita A, Haraguchi T, Hiraoka Y, Noda M (1997) **Nedd5, a mammalian septin, is a novel cytoskeletal component interacting with actin-based structures** *Genes Dev* **11**:1535–1547

65. Laporte D, Coffman VC, Lee I-J, Wu J-Q (2011) **Assembly and architecture of precursor nodes during fission yeast cytokinesis** *J Cell Biol* **192**:1005–1021

66. Lee I-J, Wu J-Q (2012) **Characterization of Mid1 domains for targeting and scaffolding in fission yeast cytokinesis** *J Cell Sci* **125**:2973–2985

67. Lee I-J, Wang N, Hu W, Schott K, Bahler J, Giddings TH, Pringle JR, Du LL, Wu JQ (2014) **Regulation of spindle pole body assembly and cytokinesis by the centrin-binding protein Sfi1 in fission yeast** *Mol Biol Cell* **25**:2735–2749

68. Lee PR, Song S, Ro HS, Park CJ, Lippincott J, Li R, Pringle JR, De Virgilio C, Longtine MS, Lee KS (2002) **Bni5p, a septin-interacting protein, is required for normal septin function and cytokinesis in Saccharomyces cerevisiae** *Mol Cell Biol* **22**:6906–6920

69. Lepore D, Spassibojko O, Pinto G, Collins RN (2016) **Cell cycle-dependent phosphorylation of Sec4p controls membrane deposition during cytokinesis** *J Cell Biol* **214**:691–703

70. Lepore DM, Martínez-Núñez L, Munson M (2018) **Exposing the Elusive Exocyst Structure** *Trends Biochem Sci* **43**:714–725

71. Li CR, Lee RT, Wang YM, Zheng XD, Wang Y (2007) **Candida albicans hyphal morphogenesis occurs in Sec3p-independent and Sec3p-dependent phases separated by septin ring formation** *J Cell Sci* **120**:1898–1907

72. Lippincott J, Li R (1998) **Sequential assembly of myosin II, an IQGAP-like protein, and filamentous actin to a ring structure involved in budding yeast cytokinesis** *J Cell Biol* **140**:355–366

73. Liu D, Li X, Shen D, Novick P (2018) **Two subunits of the exocyst, Sec3p and Exo70p, can function exclusively on the plasma membrane** *Mol Biol Cell* **29**:736–750

74. Liu J, Guo W (2012) **The exocyst complex in exocytosis and cell migration** *Protoplasma* **249**:587–597

75. Liu J, Wang H, McCollum D, Balasubramanian MK (1999) **Drc1p/Cps1p, a 1,3-beta-glucan synthase subunit, is essential for division septum assembly in Schizosaccharomyces pombe** *Genetics* **153**:1193–1203

76. Longtine MS, Bi E (2003) **Regulation of septin organization and function in yeast** *Trends Cell Biol* **13**:403–409

77. Longtine MS, DeMarini DJ, Valencik ML, Al-Awar OS, Fares H, De Virgilio C, Pringle JR (1996) **The septins: roles in cytokinesis and other processes** *Curr. Opin. Cell Biol* **8**:106–119

78. Longtine MS, Fares H, Pringle JR (1998) **Role of the yeast Gin4p protein kinase in septin assembly and the relationship between septin assembly and septin function** *J Cell Biol* **143**:719–736

79. Luo G, Zhang J, Guo W (2014) **The role of Sec3p in secretory vesicle targeting and exocyst complex assembly** *Mol Biol Cell* **25**:3813–3822

80. Marquardt J, Chen X, Bi E (2019) **Architecture, remodeling, and functions of the septin cytoskeleton** *Cytoskeleton (Hoboken* **76**:7–14

81. Martin-Cuadrado AB, Duenas E, Sipiczki M, Vazquez de Aldana CR, del Rey F (2003) **The endo-beta-1,3-glucanase eng1p is required for dissolution of the primary septum during cell separation in Schizosaccharomyces pombe** *J Cell Sci* **116**:1689–1698

82. Martin-Cuadrado AB, Morrell JL, Konomi M, An H, Petit C, Osumi M, Balasubramanian M, Gould KL, Del Rey F, de Aldana CR (2005) **Role of septins and the exocyst complex in the function of hydrolytic enzymes responsible for fission yeast cell separation** *Mol Biol Cell* **16**:4867–4881

83. Martin-Urdiroz M, Deeks MJ, Horton CG, Dawe HR, Jourdain I (2016) **The Exocyst Complex in Health and Disease** *Front Cell Dev Biol* **4**

84. McMurray MA (2019) **The long and short of membrane curvature sensing by septins** *J Cell Biol* **218**:1083–1085

85. McMurray MA, Bertin A, Garcia G, Lam L, Nogales E, Thorner J (2011) **Septin filament formation is essential in budding yeast** *Dev Cell* **20**:540–549

86. Mei K, Guo W (2018) **The exocyst complex** *Curr Biol* **28**:R922–R925

87. Mei K *et al.* (2018) **Cryo-EM structure of the exocyst complex** *Nat Struct Mol Biol* **25**:139–146

88. Meitinger F, Palani S (2016) **Actomyosin ring driven cytokinesis in budding yeast** *Semin Cell Dev Biol* **53**:19–27

89. Meitinger F, Palani S, Hub B, Pereira G (2013) **Dual function of the NDR-kinase Dbf2 in the regulation of the F-BAR protein Hof1 during cytokinesis** *Mol Biol Cell* **24**:1290–1304

90. Michaelis AC, Brunner AD, Zwiebel M, Meier F, Strauss MT, Bludau I, Mann M (2023) **The social and structural architecture of the yeast protein interactome** *Nature* **624**:192–200

91. Mirdita M, Schütze K, Moriwaki Y, Heo L, Ovchinnikov S, Steinegger M (2022) **ColabFold: making protein folding accessible to all** *Nat Methods* **19**:679–682

92. Momany M, Talbot NJ (2017) **Septins Focus Cellular Growth for Host Infection by Pathogenic Fungi** *Front Cell Dev Biol* **5**

93. Moreno S, Klar A, Nurse P (1991) **Molecular genetic analysis of fission yeast Schizosaccharomyces pombe** *Methods Enzymol* **194**:795–823

94. Mostowy S, Cossart P (2012) **Septins: the fourth component of the cytoskeleton** *Nat Rev Mol Cell Biol* **13**:183–194

95. Muñoz S, Manjón E, Sánchez Y (2014) **The putative exchange factor Gef3p interacts with Rho3p GTPase and the septin ring during cytokinesis in fission yeast** *J Biol Chem* **289**:21995–22007

96. Neubauer K, Zieger B (2021) **Role of Septins in Endothelial Cells and Platelets** *Front Cell Dev Biol* **9**

97. Neufeld TP, Rubin GM (1994) **The Drosophila peanut gene is required for cytokinesis and encodes a protein similar to yeast putative bud neck filament proteins** *Cell* **77**:371–379

98. Nishihama R, Onishi M, Pringle JR (2011) **New insights into the phylogenetic distribution and evolutionary origins of the septins** *Biol Chem* **392**:681–687

99. Oh Y, Bi E (2011) **Septin structure and function in yeast and beyond** *Trends Cell Biol* **21**:141–148

100. Oh Y, Schreiter J, Nishihama R, Wloka C, Bi E (2013) **Targeting and functional mechanisms of the cytokinesis-related F-BAR protein Hof1 during the cell cycle** *Mol Biol Cell* **24**:1305–1320

101. Onishi M *et al.* (2010) **Role of septins in the orientation of forespore membrane extension during sporulation in fission yeast** *Mol Cell Biol* **30**:2057–2074

102. Onishi M, Pringle JR (2016) **The nonopisthokont septins: How many there are, how little we know about them, and how we might learn more** *Methods Cell Biol* **136**:1–19

103. Paiano A, Margiotta A, De Luca M, Bucci C (2019) **Yeast two-hybrid assay to identify interacting proteins** *Current protocols in protein science* **95**

104. Perez AM, Finnigan GC, Roelants FM, Thorner J (2016) **Septin-Associated Protein Kinases in the Yeast Saccharomyces cerevisiae** *Front Cell Dev Biol* **4**

105. Perez P, Portales E, Santos B (2015) **Rho4 interaction with exocyst and septins regulates cell separation in fission yeast** *Microbiology* **161**:948–959

106. Petit CS, Mehta S, Roberts RH, Gould KL (2005) **Ace2p contributes to fission yeast septin ring assembly by regulating mid2+ expression** *J Cell Sci* **118**:5731–5742

107. Ren J, Guo W (2012) **ERK1/2 regulate exocytosis through direct phosphorylation of the exocyst component Exo70** *Dev Cell* **22**:967–978

108. Russell SE, Hall PA (2005) **Do septins have a role in cancer?** *Br J Cancer* **93**:499–503

109. Safavian D *et al.* (2023) **Septin-mediated RhoA activation engages the exocyst complex to recruit the cilium transition zone** *J Cell Biol* **222**

110. Santos B, Martin-Cuadrado AB, Vazquez de Aldana CR, del Rey F, Perez P (2005) **Rho4 GTPase is involved in secretion of glucanases during fission yeast cytokinesis** *Eukaryot Cell* **4**:1639–1645

111. Sharma K, Menon MB (2023) **Decoding post-translational modifications of mammalian septins** *Cytoskeleton (Hoboken* **80**:169–181

112. Sheffield PJ, Oliver CJ, Kremer BE, Sheng S, Shao Z, Macara IG (2003) **Borg/septin interactions and the assembly of mammalian septin heterodimers, trimers, and filaments** *J Biol Chem* **278**:3483–3488

113. Shen D, Yuan H, Hutagalung A, Verma A, Kümmel D, Wu X, Reinisch K, McNew JA, Novick P (2013) **The synaptobrevin homologue Snc2p recruits the exocyst to secretory vesicles by binding to Sec6p** *J Cell Biol* **202**:509–526

114. Shi W, Cannon KS, Curtis BN, Edelmaier C, Gladfelter AS, Nazockdast E (2023) **Curvature sensing as an emergent property of multiscale assembly of septins** *Proc Natl Acad Sci U S A* **120**

115. Sivaram MV, Saporita JA, Furgason ML, Boettcher AJ, Munson M (2005) **Dimerization of the exocyst protein Sec6p and its interaction with the t-SNARE Sec9p** *Biochemistry* **44**:6302–6311

116. Sjölinder M, Uhlmann J, Ponstingl H (2002) **DelGEF, a homologue of the Ran guanine nucleotide exchange factor RanGEF, binds to the exocyst component Sec5 and modulates secretion** *FEBS Lett* **532**:211–215

117. Synek L *et al.* (2021) **Plasma membrane phospholipid signature recruits the plant exocyst complex via the EXO70A1 subunit** *Proc Natl Acad Sci U S A* **118**

118. Tasto JJ, Morrell JL, Gould KL (2003) **An anillin homologue, Mid2p, acts during fission yeast cytokinesis to organize the septin ring and promote cell separation** *J Cell Biol* **160**:1093–1103

119. Tay YD, Leda M, Spanos C, Rappsilber J, Goryachev AB, Sawin KE (2019) **Fission Yeast NDR/LATS Kinase Orb6 Regulates Exocytosis via Phosphorylation of the Exocyst Complex** *Cell Rep* **26**:1654–1667

120. TerBush DR, Maurice T, Roth D, Novick P (1996) **The Exocyst is a multiprotein complex required for exocytosis in Saccharomyces cerevisiae** *EMBO J* **15**:6483–6494

121. TerBush DR, Novick P (1995) **Sec6, Sec8, and Sec15 are components of a multisubunit complex which localizes to small bud tips in Saccharomyces cerevisiae** *J Cell Biol* **130**:299–312

122. Tokhtaeva E *et al.* (2015) **Septin dynamics are essential for exocytosis** *J Biol Chem* **290**:5280–5297

123. Vallen EA, Caviston J, Bi E (2000) **Roles of Hof1p, Bni1p, Bnr1p, and myo1p in cytokinesis in Saccharomyces cerevisiae** *Mol Biol Cell* **11**:593–611

124. Vavylonis D, Wu JQ, Hao S, O'Shaughnessy B, Pollard TD (2008) **Assembly mechanism of the contractile ring for cytokinesis by fission yeast** *Science* **319**:97–100

125. Vega IE, Hsu SC (2003) **The septin protein Nedd5 associates with both the exocyst complex and microtubules and disruption of its GTPase activity promotes aberrant neurite sprouting in PC12 cells** *Neuroreport* **14**:31–37

126. Versele M, Thorner J (2005) **Some assembly required: yeast septins provide the instruction manual** *Trends Cell Biol* **15**:414–424

127. Wang H, Tang X, Balasubramanian MK (2003) **Rho3p regulates cell separation by modulating exocyst function in Schizosaccharomyces pombe** *Genetics* **164**:1323–1331

128. Wang H, Tang X, Liu J, Trautmann S, Balasundaram D, McCollum D, Balasubramanian MK (2002) **The multiprotein exocyst complex is essential for cell separation in Schizosaccharomyces pombe** *Mol Biol Cell* **13**:515–529

129. Wang N, Lee IJ, Rask G, Wu JQ (2016) **Roles of the TRAPP-II Complex and the Exocyst in Membrane Deposition during Fission Yeast Cytokinesis** *PLoS Biol* **14**

130. Wang N, Lo Presti L, Zhu YH, Kang M, Wu Z, Martin SG, Wu JQ (2014) **The novel proteins Rng8 and Rng9 regulate the myosin-V Myo51 during fission yeast cytokinesis** *J Cell Biol* **205**:357–375

131. Wang N, Wang M, Zhu YH, Grosel TW, Sun D, Kudryashov DS, Wu JQ (2015) **The Rho-GEF Gef3 interacts with the septin complex and activates the GTPase Rho4 during fission yeast cytokinesis** *Mol Biol Cell* **26**:238–255

132. Werner B, Yadav S (2023) **Phosphoregulation of the septin cytoskeleton in neuronal development and disease** *Cytoskeleton (Hoboken* **80**:275–289

133. Wloka C, Nishihama R, Onishi M, Oh Y, Hanna J, Pringle JR, Krauss M, Bi E (2011) **Evidence that a septin diffusion barrier is dispensable for cytokinesis in budding yeast** *Biol Chem* **392**:813–829

134. Woods A, Sherwin T, Sasse R, MacRae TH, Baines AJ, Gull K (1989) **Definition of individual components within the cytoskeleton of Trypanosoma brucei by a library of monoclonal antibodies** *J Cell Sci* **93**:491–500

135. Woods BL, Gladfelter AS (2021) **The state of the septin cytoskeleton from assembly to function** *Curr Opin Cell Biol* **68**:105–112

136. Wu J-Q, Kuhn JR, Kovar DR, Pollard TD (2003) **Spatial and temporal pathway for assembly and constriction of the contractile ring in fission yeast cytokinesis** *Dev Cell* **5**:723–734

137. Wu J-Q, Ye Y, Wang N, Pollard TD, Pringle JR (2010) **Cooperation between the septins and the actomyosin ring and role of a cell-integrity pathway during cell division in fission yeast** *Genetics* **186**:897–915

138. Yang L, Zhang X, Gu Y, Shi Y, Wang LB, Shi JX, Zhen XX, Xin YW, Gu WW, Wang J (2022) **SEC5 is involved in M2 polarization of macrophages via the STAT6 pathway, and its dysfunction in decidual macrophages is associated with recurrent spontaneous abortion** *Front Cell Dev Biol* **10**

139. Ye Y, Lee I-J, Runge KW, Wu J-Q (2012) **Roles of putative Rho-GEF Gef2 in division-site positioning and contractile-ring function in fission yeast cytokinesis** *Mol Biol Cell* **23**:1181–1195

140. Yin R, Pierce BG (2023) **Evaluation of AlphaFold Antibody-Antigen Modeling with Implications for Improving Predictive Accuracy** *bioRxiv*

141. Yue P, Zhang Y, Mei K, Wang S, Lesigang J, Zhu Y, Dong G, Guo W (2017) **Sec3 promotes the initial binary t-SNARE complex assembly and membrane fusion** *Nat Commun* **8**

142. Zhang L, Cai Y, Li Y, Zhang T, Wang B, Lu G, Zhang D, Olsson S, Wang Z (2021) **MoSep3 and MoExo70 are needed for MoCK2 ring assembly essential for appressorium function in the rice blast fungus, Magnaporthe oryzae** *Mol Plant Pathol* **22**:1159–1164

143. Zhang XM, Ellis S, Sriratana A, Mitchell CA, Rowe T (2004) **Sec15 is an effector for the Rab11 GTPase in mammalian cells** *J Biol Chem* **279**:43027–43034

144. Zheng S, Dong F, Rasul F, Yao X, Jin QW, Zheng F, Fu C (2018) **Septins regulate the equatorial dynamics of the separation initiation network kinase Sid2p and glucan synthases to ensure proper cytokinesis** *Febs j* **285**:2468–2480

145. Zheng S, Zheng B, Fu C (2024) **The Roles of Septins in Regulating Fission Yeast Cytokinesis** *J Fungi (Basel* **10**

146. Zhou TT, Zhao YL, Guo HS (2017) **Secretory proteins are delivered to the septin-organized penetration interface during root infection by Verticillium dahliae** *PLoS Pathog* **13**

147. Zhu YH, Hyun J, Pan YZ, Hopper JE, Rizo J, Wu JQ (2018) **Roles of the fission yeast UNC-13/Munc13 protein Ync13 in late stages of cytokinesis** *Mol Biol Cell* **29**:2259–2279

148. Zhu YH, Ye Y, Wu Z, Wu JQ (2013) **Cooperation between Rho-GEF Gef2 and its binding partner Nod1 in the regulation of fission yeast cytokinesis** *Mol Biol Cell* **24**:3187–3204

Editors

Reviewing Editor
Mohan Balasubramanian
University of Warwick, Coventry, United Kingdom

Senior Editor
Felix Campelo
Institute of Photonic Sciences, Barcelona, Spain

Reviewer #1 (Public Review):

Summary:
In this manuscript, Singh, Wu and colleagues explore functional links between septins and the exocyst complex. The exocyst in a conserved octameric complex that mediates the tethering of secretory vesicles for exocytosis in eukaryotes. In fission yeast cells, the exocyst is necessary for cell division, where it localizes mostly at the rim of the division plane, but septins, which localize in a similar manner, are non-essential. The main findings of the work are that septins are required for the specific localization of the exocyst to the rim of the division plane, and the likely consequent localization of the glucanase Eng1 at this same location, where it is known to promote cell separation. In the absence of septins, the exocyst still localizes to the division plane but is not restricted to the rim. They also show some defects in the localization of secretory vesicles and glucan synthase cargo. They further propose that interactions between septins and exocysts are direct, as shown through Alphafold2 predictions (of unclear strength) and clean coIP experiments.

Strengths:
The septin, exocyst and Eng1 localization data are well supported, showing that the septin rim recruits the exocyst and (likely consequently) the Eng1 glucanase at this location. One major finding of the manuscript is that of a physical interaction between septins and exocyst subunits. Indeed, many of the coIPs supporting this discovery are very clear.

Weaknesses:
I am less convinced by the strength of the physical interaction of septins with the exocyst

complex. Notably, one important open question is whether septins interact with the intact exocyst complex, as claimed in the text, or whether the interactions occur only with individual subunits. The two-hybrid and coIP data only show weak interactions with individual subunits, and some coIPs (for instance Sec3 and Exo70 with Spn1 and Spn4) are negative, suggesting that the exocyst complex does not remain intact in these experiments. Given the known structure of the full exocyst complex and septin filaments (at least in S. cerevisiae), the Alphafold2 predicted structure could be used to probe whether the proposed interaction sites are compatible with full complex formation.

The effect of spn1Δ on Eng1 localization is very clear, but the effect on secretory vesicles (Ypt3, Syb1) and glucan synthase Bgs1 is less convincing. The effect is small, and it is not clear how the cells are matched for the stage of cytokinesis.

https://doi.org/10.7554/eLife.101113.1.sa2

Reviewer #2 (Public Review):

Summary:
This interesting study implicates the direct interaction between two multi-subunit complexes, known as the exocyst and septin complexes, in the function of both complexes during cytokinesis in fission yeast. While previous work from several labs had implicated roles for the exocyst and septin complexes in cytokinesis and cell separation, this study describes the importance of protein:protein interaction between these complexes in mediating the functions of these complexes in cytokinesis. Previous studies in neurons had suggested interactions between septins and exocyst complexes occur but the functional importance of such interactions was not known. Moreover, in baker's yeast where both of these complexes have been extensively studied - no evidence of such an interaction has been uncovered despite numerous studies which should have detected it. Therefore while exocyst:septin interactions appear to be conserved in several systems, it appears likely that budding yeast are the exception--having lost this conserved interaction.

Strengths:
The strengths of this work include the rigorous analysis of the interaction using multiple methods including Co-IP of tagged but endogenously expressed proteins, 2 hybrid interaction, and Alphafold Multimer. Careful quantitative analysis of the effects of loss of function in each complex and the effects on localization and dynamics of each complex was also a strength. Taken together this work convincingly describes that these two complexes do interact and that this interaction plays an important role in post Golgi vesicle targeting during cytokinesis.

Weaknesses:
The authors used Alphafold Multimer to predict (largely successfully) which subunits were most likely to be involved in direct interactions between the complexes. It would be very interesting to compare this to a parallel analysis on the budding yeast septin and exocyst complexes where it is quite clear that detectable interactions between the exocyst and septins (using the same methods) do not exist. Presumably the resulting pLDDT scores will be significantly lower. These are in silico experiments and should not be difficult to carry out.

https://doi.org/10.7554/eLife.101113.1.sa1

Reviewer #3 (Public Review):

Septins in several systems are thought to guide the location of exocytosis, and they have been found to interact with the exocyst vesicle-tethering complex in some cells. However, it is not known whether such interactions are direct or indirect. Moreover, septin-exocyst physical

associations were not detected in several other systems, including yeasts, making it unclear whether such interactions reflect a conserved septin-exocytosis link or whether they may missed if they depend on septin polymerization or association into higher-order structures. Singh et. al., set out to define whether and how septins influence the exocyst during S. pombe cytokinesis. Based on three lines of evidence, the authors conclude that septins directly bind to exocyst subunits to regulate localization of the exocyst and vesicle secretion during cytokinesis.
The conclusions are consistent with the data presented, but some interpretations need to be clarified and extended:

(1) The first line of evidence examines septin and exocyst localization during cytokinesis in wild-type and septin-mutant or exocyst-mutant yeast. Quantitative imaging convincingly shows that the detailed localization of the exocyst at the division site is perturbed in septin mutants, and that this is accompanied by modest accumulation of vesicles and vesicle cargos. Whether that is sufficient to explain the increased thickness of the division septum in septin mutants remains unclear.

(2) The second line of evidence involves a comprehensive Alphafold2 analysis of potential pair-wise interactions between septin and exocyst subunits. This identifies several putative interactions in silico, but it is unclear whether the identified interaction surfaces would be available in the full septin or exocyst complexes.

(3) The third line of evidence uses co-immunoprecipitation and yeast two hybrid assays to show that several physical interactions predicted by Alphafold2 can be detected, leading the authors to conclude that they have identified direct interactions. However, both methods leave open the possibility that the interactions are indirect and mediated by other proteins in the fission yeast extract (co-IP) or budding yeast cell (two-hybrid).

(4) Based on prior studies it would be expected that the large majority of both septins and exocyst subunits are present in cells and extracts as stoichiometric complexes. Thus, one would expect any septin-exocyst interaction to yield associations detectable with multiple subunits, yet co-IPs were not detectded in some combinations. It is therefore unclear whether the interactions reflect associations between fully-formed functional complexes or perhaps between transient folding intermediates.

https://doi.org/10.7554/eLife.101113.1.sa0